This is a peer-reviewed, accepted author manuscript of the following research article: Haq, M. A. U., Hussain, S., Ali, M. A., Farooq, M. U., Mufti, N. A., Pruncu, C. I., & Wasim, A. (Accepted/In press). Evaluating the effects of nano fluids based MQL milling of IN718 associated to sustainable productions. *Journal of Cleaner Production*.

Evaluating the effects of nano fluids based MQL milling of IN718 associated to sustainable productions

Muhammad Ahsan ul Haq[a], Salman Hussain[a], Muhammad Asad Ali[a,b*], Muhammad Umar Farooq[b,c*], Nadeem Ahmad Mufti[b], Catalin I. Pruncu[d,e*], Ahmad Wasim[a]

[a]Department of Industrial Engineering, University of Engineering and Technology, Taxila 47080, Pakistan; ahsanulhaq233@gmail.com (M. A. H.); salman.hussain@uettaxila.edu.pk (S. H.); wasim.ahmad@uettaxila.edu.pk (A. W.)

[b]Department of Industrial and Manufacturing Engineering, University of Engineering and Technology, Lahore 54890, Pakistan; namufti@uet.edu.pk (N. A. M.)

[c]Department of Industrial and Systems Engineering, Korea Advanced Institute of Science and Technology, Daejeon 34141, Korea

[d]Mechanical Engineering, Imperial College London, Exhibition Rd., SW7 2AZ, London, UK;

[e]Design, Manufacturing & Engineering Management, University of Strathclyde, Glasgow, G1 1XJ, Scotland, UK.

***Corresponding authors:** asad.ali@uet.edu.pk (M. A. A.); Umarmuf0@gmail.com (M.U.F.); Catalin.pruncu@strath.ac.uk (C. I. P.)

Abstract

The aeronautical industry is constantly striving for goals related to lesser production/maintenance time and cost. In this regard, aero-engines made up of Nickel-based alloy are preferred for high performance to improve the burning efficiency. However, the processing of the Nickel-based alloys remain challenging in manufacturing industry with the aim of sustainable production. This research investigated the manufacturing progress of face milling of Inconel 718 by using two different lubrication conditions; minimum quantity lubrication (MQL) and nanofluids based minimum quantity lubrication (NF-MQL). A high degree of sustainability was achieved through increasing productivity (material removal rate) and quality (surface roughness) enhancement while minimizing the power and temperature. The impacts of four most influencing parameters including feed rate, speed, flow rate and depth of cut were investigated on sustainable production performance measures. Empirical models of surface roughness, temperature, material removal rate and power were developed using response surface methodology. Analysis of the developed empirical models and validation were executed through analysis of variance and confirmatory experiments results. Finally, a multi objective optimization was implemented to attain maximum sustainability effect by generating a compromise between lowest surface roughness and cost, and highest material removal rate. The results revealed that the depth of cut is the most significant process parameter for both lubrication environments. The results show the NF-MQL as the better alternative which resulted in 20.1%, 14.7% and 13.3% percentage reduction for surface roughness, temperature and power, respectively. Furthermore, the results revealed that NF-MQL resulted in better desirability achievement (71.3%) as compared to MQL (70.1%).

Keywords: Minimum Quantity Lubrication, Nanofluids, Inconel 718, surface roughness, Sustainability

1. Introduction

Nickel-based superalloys are being employed in the aeronautical sector for specialized purposes because of their excellent serviceability qualities. In these alloys, Inconel 718 is very famous for its higher strength-to-weight ratio, superior corrosion resistance, performance capability at elevated temperatures along with thermal fatigue resistance and good strain-hardening characteristics [1]. Considering aeronautical applications, the major goals in the industry include lesser time and cost, and better convenience while moving between places [2]. To achieve these formidable goals, aforesaid superalloys are strengthening the aviation manufacturing industry with the focus to reduce fuel costs and improve burning efficiency. The fuel consumption and emission levels are highly dependent on the material which is used in aero-engine. Therefore, Nickel-based superalloy (Inconel 718) provides the opportunity for better fuel burning to ensure maximum engine temperature possibility due to the capability of retaining mechanical properties at elevated temperatures [3]. It is also used in marine and nuclear reactor equipment.

Concentrating on the highly specialized applications, machinability challenges also come with the intrinsic properties of the alloy. The dilemma associated with the machining of Inconel 718 is its low thermal conductivity which prevents efficient heat dissipation heading to rise in the tool wear when the heat energy at the point of contact increases [4]. Therefore, strong adhesion of material and tool is developed during machining causing shoddier machinability [5]. Due to these deficiencies, the industry is enforced to the trade-off between the manufacturing cost and work quality under sustainable production challenges [6]. Several studies are conducted on improving work quality (roughness) and machining efficiency (material removal rate) of Inconel 718 machining through a lot of the assistive technologies. To improve surface integrity and minimize temperature generation during machining, many cooling systems are employed in conventional machining processes [7]. The use of flood cooling is beneficial in reducing friction and process temperature [8]. On contrary to this, dry cooling comes with the advantage of environmental consciousness and safety for machinists from the diseases possibly caused by cutting fluids (CF) [9]. The sustainability challenge to reduce energy, tooling and work quality cost during dry machining, improvements are used in the process using near-dry, spray technology, MQL, NF-MQL and cryogenic technology [10].

MQL and NF-MQL are deemed to be the greener [11], eco-benign and socio-economic substitute of dry and flood cooling technologies [12]. Manufacturing industries have started focusing on sustainable production and environmental obligation which makes afore-cited techniques preferable [13]. Nanofluids have better cooling and lubrication actions than pure and flood cooling effects [14] because of the formation of strong lubrication films during machining. Also, NFs can penetrate better into the surface because of the pressure

of the MQL technique, reduces the cutting forces that lead to better lubrication [15]. Gupta et al. [16] studied the life cycle cost associated with MQL based turning of pure titanium. The study has reported that MQL serves as a sustainable cooling condition with reverence to machining performance, economic concerns and energy consumption. Moreover, surface roughness is significantly influenced by cooling conditions while no remarkable difference is observed on the material removal rate because of its high dependence on cutting speed, feed rate and depth of cut. Khan et al. [17] investigated sustainability and energy-based cost during turning of AISI 52100 steel using MQL, NF-MQL, hybrid NF-MQL based cooling conditions. Two types of particles, Al_2O_3 and graphene nanoparticles have been mixed for the nanofluids evaluation on machining. The study has demonstrated that hybrid NF-MQL is better as compared to MQL in producing good surface quality. Additionally, cutting and machining power are influenced by cutting speed in all lubrication approaches. Hybrid NF-MQL has produced better results in optimizing machining power-based cost as compared to other lubrication conditions. Abellan-Nebot et al. [18] compared air cooling, dry and MQL lubrication approach on surface roughness (SR) and power consumption (P_C) in the manufacturing of molds. In addition to this study, the lubricant flow rate in MQL is an influential factor in controlling the responses. The overall evaluation concluded that MQL is found auspicious in terms of machining cost and economic aspects than the conventional cooling approaches. Wang et al. [19] investigated three NF-MQL conditions (palm oil, MoS_2, Al_2O_3) on the grinding process. In this work, palm oil developed a physical thin oil layer exhibiting poor anti-wear, friction performance and affected stability during severe grinding processes. On the other side, NF-MQL generated a tribo-film which improved surface through reducing friction. Several studies evaluate the potentiality of MQL and NF-MQL approaches for improving machining efficiency, work quality, environmental and operators health focus. Likewise, These approaches are found promising for the machining of difficult-to-cut materials such as Ni and Ti alloys to produce sustainable and optimal results. The complexity comes with the advantages of proper preparation and stability of nanofluids [10].

In the aforementioned perspective, work is available with a focus on the milling process. The process is preferred due to producing shape variety for different applications [20] and improved surface finish, reducing energy consumption and temperature produced during machining. Moreover, appropriate parameters amalgamation with well-arranged machining setup is considered to yield amazing results [21]. Hence, the challenge lies in determining the significance of process parameters on various responses which directly or indirectly affect the performance of afore-cited industrial applications and cause economic concerns. Do and Le [22] found that depth of cut and feed rate are the most influential parameters on SR in milling of H13 steel under MQL conditions. Moreover, the study reported that the depth of the cut is directly proportional to the cutting forces produced. Jebaraj et al. [21] investigated milling process parameters on cutting forces, temperature and SR of Al6082-T6 alloy. Analysis of variance

(ANOVA) resulted in that lubrication environment (72.07%), feed rate (12.20%) and cutting speed (4.28%) were found significant on response indicators. Singh et al. [23] established that MQL is a better environment than the flood and dry milling of Inconel 718 in the context of tool degradation costs. The study resulted that cutting speed was the vital influencing variable in determining tool life. The investigation suggested evaluating NF-MQL on temperature and surface morphology produced during machining of Inconel 718. Varghese et al. [24] optimized milling process parameters under the cryogenic cooling condition for machining of AISI 304 and obtained 0.25 μm surface roughness as a minimum.

Along with optimizing process parameters, the significance of CF used in the milling process cannot be underestimated within actual environmental and economic framework [25]. Different fluids such as air, gases, water, oil-based emulsions and additive mixed serve as cooling and lubricating necessities [26]. Adequate flushing medium volume and fluid type help in removing chips, reducing chances of tool and workpiece corrosion [27]. From the available literature, it is evident that almost all traditional machining oils have rapid evaporation or decomposition rates which contribute to serious environmental concerns in terms of hazardous health effects and environmental pollution [28]. The rationale behind the usage of distilled water is due to its capacity of being eco-friendly, biodegradability, free from heavy metals as compared to oil-based lubrications which are more toxic and non-biodegradability [29]. To address this issue, vegetable and other bio-oils are used contributing to a significant portion of the cost. Therefore, water and water-based nano-fluids are capable of taking in as more sustainable and eco-friendly CF considering harmfulness and non-biodegradability of other fluids. For NF-MQL, there are two types of nanofluids used in different machining processes, for instance, metallic and non-metallic nanofluids due to their superior thermal and reduction in friction qualities. In metallic nanofluids, Cu based nanofluid is commonly used due to its decisive role in thermal conductivity enhancement. It has shown 78% higher thermal conductivity which classify it as one of the highest in the nanofluids [30]. During the milling of Al-alloy, water-based TiO_2 nanofluid produced supportable results as compared to water only. It was found beneficial to integrate higher cooling rates of water to nanoparticles for performance enhancement [29]. Subsequent homogenization and adequate dispersion of nanoparticles, to restrain from agglomeration are necessary, to effectively get the benefit of the technology [31].

Generally, CF are carried through nozzles just like flooded CF in machining processes. They trigger higher manufacturing and nanofluids/CF costs and continuously urge numerous researchers to explore the optimal settings and potentiality of different CF integrated with MQL/NF-MQL conditions to aid in the machining [32]. The use of different CF in MQL as a sustainable manufacturing technique and the use of nanoparticles in conventional CF to improve machining efficiency were scarce, noted in the literature . In past, the major focus has been on reducing surface roughness and improving machining efficiency but very few researches on sustainability indicators. In most cases, conventional roughing and finishing through

milling is suggested. Also, very limited research is available on using water and water-based nanofluids with superior focus on greener production. To further improve the state of art, there is a major need for a comprehensive investigation on the evaluation of flow rate and effect on industrial sustainability indicators in water-based MQL/NF-MQL on Inconel 718 for aerospace applications.

In this research, to obtain sustainable production in face milling of Inconel 718, two different lubrication conditions (MQL and NF-MQL) are thoroughly investigated. This has been achieved through machining efficiency (material removal rate: MRR) and quality (surface roughness: SR) enhancement simultaneously by minimizing the cost (power and temperature). Further, a mechanistic understanding of the surface characteristics evolution during the MQL and NF-MQL machining using the water-based Cu nanofluid which is a demanding task for industry was carefully presented in this work.

It leads to an environmental solution and cost-effective option for the manufacturing sector. The undertaken research explores scientific phenomenon by investigating the effects of four most influencing parameters; feed rate, speed, flow rate and depth of cut on sustainable production performance measures during face milling on IN718. It also tries to evaluate the surface characteristics of MQL and NF-MQL machining using the water-based Cu nanofluid under the efficiency-quality-cost nexus. Further, it optimizes the process parameters based on sustainability indicators evaluated during machining of the Inconel 718 by using Cu nanofluid. Furthermore, this work provides an insight on physical phenomenon of MQL and NF-MQL that has major effects on material removal, power consumption and tool-workpiece interaction temperature. The research study will open a new window in the aviation industry by integrating the understanding of water-based sustainable lubrication, and minimum quantity-based effective lubrication technique. Hence, an appopiate sustainability process leads in achieving the best lubrication condition which results in improved work quality, efficient and better economical performance. The manufacturing cost will be significantly reduced without compromising the process robustness and alloy properties.

2. Materials and methods

2.1 Work material, machine and cutting tool

In this study, Nickel-based superalloy Inconel 718 is used as a workpiece. It possesses exceptional thermo-mechanical properties which make it preferable in highly specialized applications in aerospace and other defence industries. The salient properties of the workpiece include serviceability at elevated performance conditions and temperature, high corrosion resistance and low thermal conductivity. The element-based composition of the Inconel 718 alloy is confirmed from manufacturer's quality sheet showing composition as Ni (54.3%), Cr (19.7%), Fe (15.5%), Mo (3%), Al (0.95%), Nb (4.79%), C (0.08%) and Si (0.35%), which

was further verified through energy-dispersive X-ray spectroscopy (model: Impect S50, USA) (see Fig. 1). The superior properties making Inconel 718 the most desirable are mentioned in Table 1. The workpiece samples having dimensions $100 \times 50 \times 8$ mm^3 (Length × Width × Thickness) were used during the experimentation.

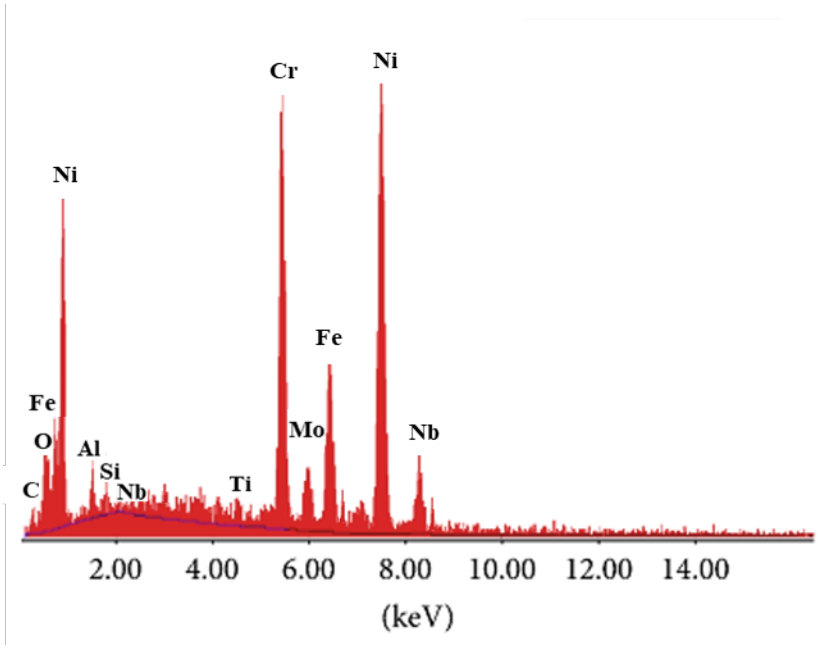

Figure 1. EDAX based elemental composition of IN718.

As this material is subjected to specialized applications having superior surface finish, therefore it is commonly machined through the milling process. Hence, Milling tests were conducted at CNC Machining Center (model MCV600, Long Chang, Taiwan) having spindle speed range of 8000 rev/min and rated power of 20 kVA. Moreover, square-shaped carbide inserts were used (as cutting insert) for machining of the workpiece. Face milling was carried out with the help of PVD ALTICRN coated CoroMill® 415 insert (ISO code: 415N-07 03 20M-M30 1130) hold in an insert holder or tool (CoroMill® 415 face milling cutter ISO code: 415-032A25-07H) having 5 number of teeth. Tool having a diameter of 20.5 mm used for this purpose. Insert had inscribed circle diameter 7 mm, cutting edge effective length 3 mm, corner chamfer width 0.1 mm, wiper edge radius 2 mm, a corner radius 2 mm, corner radius equivalent 2.8 mm, major cutting edge angle 15°, face land width 0.1 mm, face land angle 5° and insert thickness 3.07 mm.

Table 1. The prominent properties of workpiece [33]

Mechanical properties		**Thermal properties**	
Ultimate strength (MPa)	1260-1390	Thermal conductivity (W/m K)	10-11
Yield point (MPa)	1041-1160	Melting point (°C)	1350
Poisson's ratio	0.25-0.35		
Elongation (%)	14-19		
Hardness (HRC)	44		

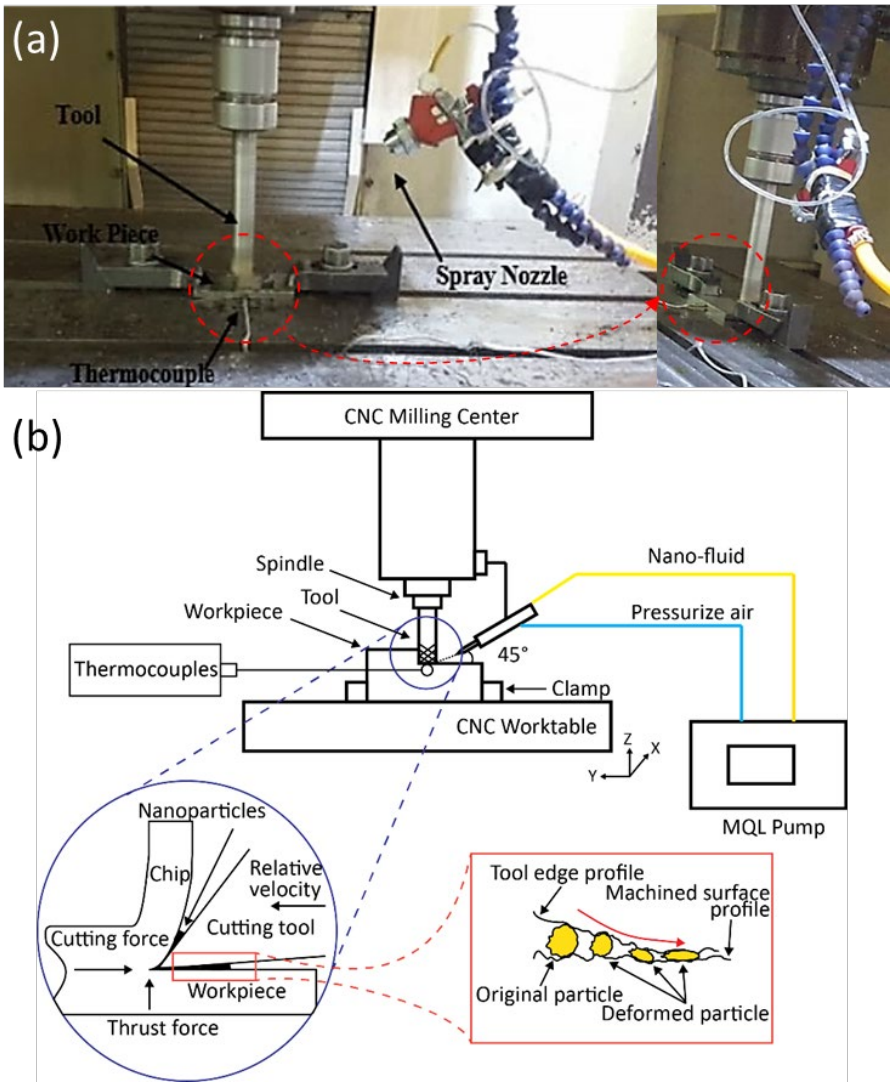

Figure 2. (a) Experimental setup for NF-MQL milling condition (b) Schematic illustration of the NF-MQL milling process

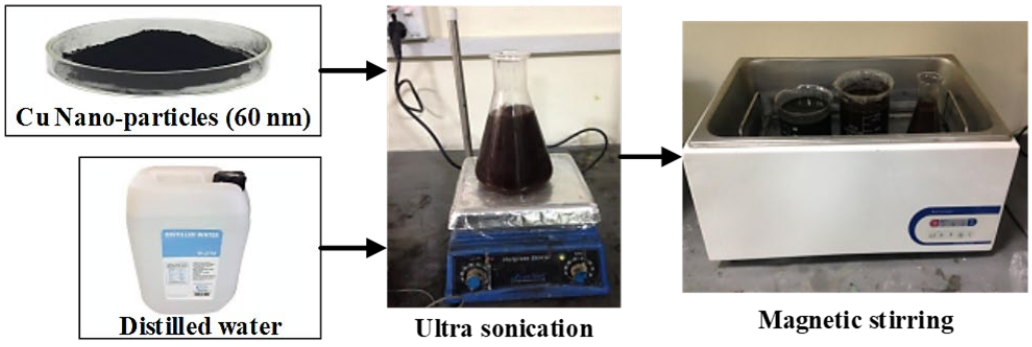

Figure 3. Cu-Nanofluid preparation of by the two-step mixing method

2.2 MQL and the preparation of the nanofluid

An experiment-based investigation was carried out in two lubrication conditions such as MQL (0% nanofluid concentration) and NF-MQL. To carry out the experiments, MQL pump (LubriLean Vario type) of the SKF company was utilized. The MQL supply parameters used as constant are gas-liquid ratio 0.4, and liquid flow rate 0.005 kg/s. Different flow rates were investigated while constant air pressure of 4 bar was maintained to adequately spray lubricant with the help of nozzle oriented at an angle of 45° to the surface of the workpiece (as advocated by Ross and Manimaran [34]) and nozzle distance of 25 mm as optimized for better functionality [35]. For NF-MQL, Cu based nanofluid is used because of its potential for thermal conductivity enhancement and reduction in friction qualities. Therefore, Cu nanoparticles were used having a nominal diameter of ~60 nm. To avoid agglomeration of nanoparticles, surfactants are used in the case of oils for ensuring dispersion [36]. However, surfactant-free copper distilled water-based nanofluid with anti-corrosive agent (as per recommendation of Kole and Dey [31]) having a concentration of Cu nanoparticles 0.2% (volume fraction) was set with proper and uniform dispersion through intense ultrasonication using a 200 W Ultra Sonicator (model UP200S, Ms. Hielscher GmBH) for 120 min. In last, nanofluid was mixed through magnetic stirring for 60 min (Fig. 3). The experimental setup used for the experimentation under both conditions of MQL and NF-MQL has been shown in Fig. 2(a). The graphic representation of the process has been provided in Fig. 2(b) depicts the overall process. The process science is illustrated to show how nano-particles interact between both faces reducing the friction as well as temperature. Fig. 2(b) demonstrated the machining nanofluid supply in the NF-MQL milling process. Air compressor atomized the nanofluid in a nozzle and changed it into very fine mist (nanoparticle crammed by water film for water-based nanofluid). Mist can pass in the shearing region sustaining the gap between tool-workpiece and chip fractured channels to lubricate the contact region since the velocity of mist is higher than the rotational speed of milling tool as depicted in Fig. 2(b). The nano-particles in the cutting region origin the formation of a tribo-film because water-based nanofluid mist deposited the nano-particles on the surface of cutting tool-workpiece. Development of tribo-film enhanced the lubrication effect in the shearing region that resulted in lower frictional shear stress and reduced the tangential cutting force.

2.3 Experimental design and cutting conditions

The input control variables selected for the experiments were feed rate, speed, flow rate and depth of cut [20] due to their established pivotal role witnessed from the literature [37, 38] for better understanding of the process [38]. Moreover, their ranges have been identified and tested by taking the basis of previous research [35] on the milling of nickel-based superalloys [7] and other materials of similar hardness. Initially, 9 trail experiments were carried out to ensure righteousness of functioning setup and workability

in the range of input parameters. Keeping the axial depth of cut as input variable, radial depth of cut was taken as constant 12 mm. The variables along with their levels and response indicators are stated in Table 2.

A design of experiment approach (DOE) was used to understand critical factors promoting consequences on sustainability indicators (material removal rate: MRR, surface roughness: SR, temperature: T and power consumption: P_C). Central composite design (CCD) was used for developing empirical models and analysis of all responses [37]. In response surface methodology (RSM) based CCD approach, if the number of process variables and center points is represented by "k" and "m' respectively, then the total number of runs "n" can be obtained by the Eq. 1.

$$n = 2^k + 2k + m \qquad (1)$$

For this research, thirty experiments have been designed and conducted using four process parameters and six center points. The complete design was repeated for both lubrication approaches (MQL and NF-MQL). In total 69 experiments were performed. The 30 experiments are carried out against MQL and NF-MQL setups each.

Table 2. Input variables and their levels in RSM based DOE and response indicators

	Level	Speed (rpm) S_P	Feed rate (mm/min) F_R	Axial depth of cut (mm) D_{OC}	Flow rate (ml/hr) Fl_R
Input process parameters	+1	3000 (193 m/min)	80	0.80	800
	0	2500 (161 m/min)	55	0.55	600
	-1	2000 (129 m/min)	30	0.30	400
	Response indicator		**Symbol**	**Units**	
Performance measures	Surface roughness		SR	µm	
	Temperature		T	°C	
	Material removal rate		MRR	mm^3/min	
	Power consumption		P_C	Watt	

2.4 Response measurements

Shearing on the primary plane and tool-workpiece friction generates the temperature of vital importance. This contributes to a different type of tool degradation phenomena for instance diffusive wear, abrasive wear and adhesive wear [38]. Data acquisition system with k type thermocouple (temperature range from -200 to 1250°C) and signal conditioning unit 'Max6675' was used for measuring temperature during machining. For accurate measurement of temperature, the thermocouple was implanted into the workpiece at about 0.3 mm below the new generated surface (as per guidelines by Kim et al. [39]). The thermocouple was attached in the workpiece by making a hole (0.5 mm diameter) as shown in Fig. 2, which

were positioned at the spindle axis of the milling cutter. The thermocouple interacted with one side in workpiece hole towards the cutting region (heat affected zone (HAZ)), so that this arrangement precisely measures the temperature during machining.

Surface Texture meter (model Surtronic S-100, Taylor Hobson, USA) having a portable stylus was utilized to measure the work roughness-SR. The direction of surface roughness measurement was perpendicular to cutting lay using standard gaussian filter (EN ISO 16610-21). Ra values were recorded and used for analysis because of their wide acceptability in industry. The experimental material removal rate was calculated using Eq. 2.

$$\mathrm{MRR} = \frac{W_{bm} - W_{am}}{t_m \times \rho_w} \qquad (2)$$

In Eq. 2, W_{bm} and W_{am} are the weight of the workpiece before and after machining, correspondingly. The machining time is represented by t_m which is measured while engaging parametric conditions for specified cutting length discontinuing idle period (as per guidelines by Sealy et al. [40]) and density of workpiece is shown as ρ_w. Power consumed in machining was noted by three-phase power sensor (WB9128-1) with the capacity to gauge low voltage systems up to 380 V conductor to earth and currents up to 40 A in the used arrangement. Similar power measuring setup was utilized in another study [41]. The responses are measured more than three times to ensure the reliability and to exclude variability.

3. Results and discussions

3.1 Parametric effect analysis

The effects of varying feed rate, speed, depth of cut and flow rate on the surface roughness, temperature, material removal rate and power for both the lubrication environment have been analyzed using 3D response surface plots.

3.1.1 Response surface plots for surface roughness

Fig. 4a and Fig. 4d demonstrate the influences of S_P and D_{OC} on surface roughness for MQL and NF-MQL lubrication conditions, respectively. By comparing these plots, it is evident that the impacts of varying S_P and D_{OC} on work roughness are similar. Worksurface quality is more sensitive to the deviation of D_{OC} than S_P [42]. Furthermore, surface roughness declines with the increment in S_P up to a certain level. With the further enhancement in S_P, surface roughness increases. Furthermore, SR also increases with a rise in D_{OC}. It is worthy to mention that lowest surface roughness has been achieved for NF-MQL lubrication environment. The influences of D_{OC} and F_R on the roughness for MQL and NF-MQL have been presented in Fig. 4b and Fig. 4e respectively. It is examined that surface roughness is lowest at low levels of D_{OC} and F_R, whereas, it is maximum at high levels of D_{OC} and F_R. The science behind the fact is that high F_R stimulates

the induction of high cutting forces at the chip, tool and workpiece interaction zone. When F_R and cutting speed are enhanced, high vibration and temperature are generated in the cutting region, subsequently leading to higher SR. Furthermore, the effects of D_{OC} on surface roughness are very large as compared to F_R. Fig. 4c and Fig. 4f depicts the effects of D_{OC} and Fl_R for both the environments. It is found that surface roughness significantly rises with increment in D_{OC}, while declines slightly with addition in Fl_R [43]. Moreover, with an addition of nanoparticles enhance the thermal conductivity of the fluid and it also initiates the rolling effect that causes the reduction of friction between the interaction point of the tool and the workpiece. Thus, lesser tool flank wears throughout milling ultimately improving the work quality [42]. The phenomenon involved the abrasive grains between the tool and the workpiece may was responsible for the reduction in surface roughness. Moreover, a good surface finish is attained by an excellent cooling environment that removes chips from the tool surface [44]. Furthermore, the formation of good chip quality causes a decline in roughness. Additionally, the ball-bearing effect of rolling nanoparticles forms a mist that reduces friction in the machining zone [45].

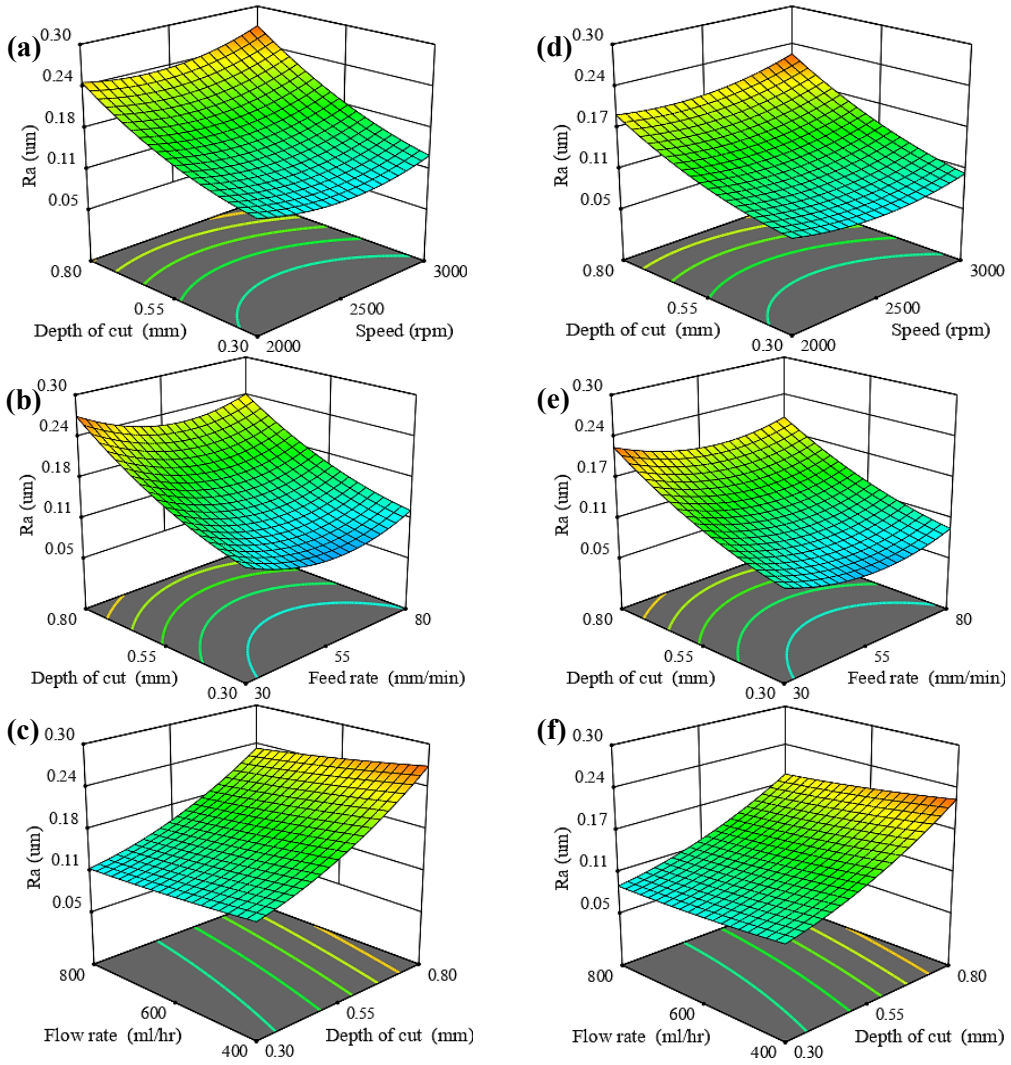

Figure 4. Response surface plots showing the parametric effects on surface roughness for (a-c) MQL, (d-f) NF-MQL lubrication environment

3.1.2 Response surface plots for temperature

The rationale behind considering temperature as a response is because it influences tool life, machinability and quality of the surface significantly [46]. The 3D plots illustrated the influences of S_P and D_{OC} on temperature for MQL lubrication environment (Fig. 5a) is similar to NF-MQL lubrication environment (Fig. 5d). The response surface plots indicate the direct influence of S_P and D_{OC} on temperature. It can also be examined that temperature is affected more by D_{OC} than speed. Furthermore, the temperature rises with addition in D_{OC}. When comparing the effects of F_R and D_{OC} on temperature under MQL and NF-MQL lubrication environments, similar trends can be observed (Fig. 5b and Fig. 5e). Effect of D_{OC} is more as compared to F_R due to shear phenomenon. A slight increase in temperature is observed with increment in feed rate; however, the temperature rises significantly with D_{OC}. The effects of D_{OC} and Fl_R on temperature have been shown in Fig. 5c and Fig. 5f. For both lubrication environments, the combination of minimum D_{OC} and maximum Fl_R results in the lowest temperature value. Furthermore, the temperature rises with addition in D_{OC} and decreases with increase in Fl_R. Concerning this point, some research contributes to this phenomenon, to the synthetic and complex impact of vibration and cutting temperature in milling [47].

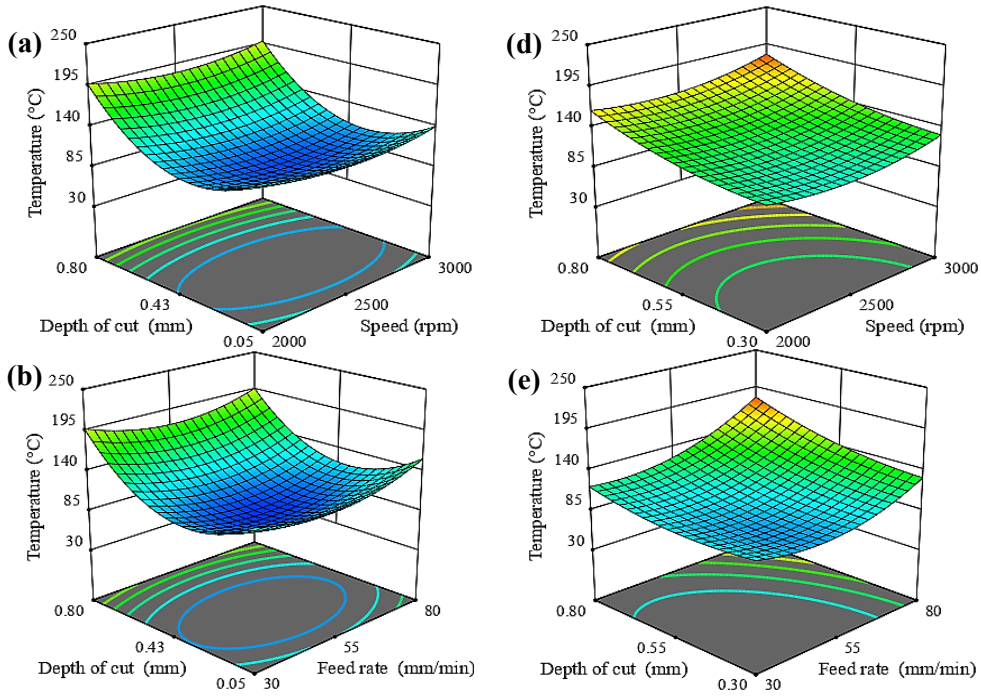

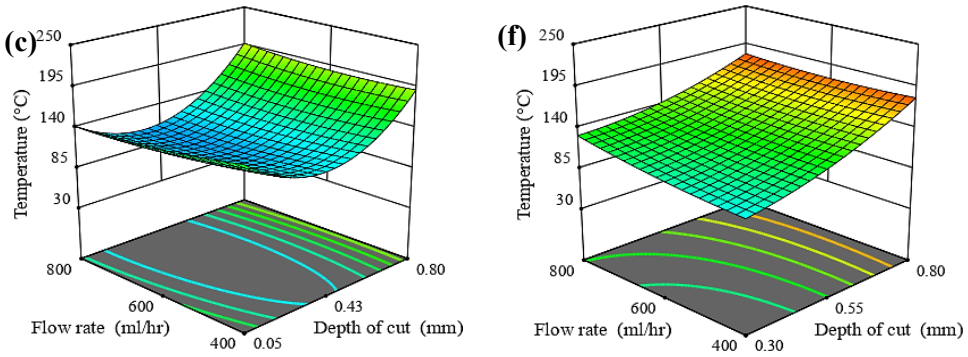

Figure 5. Response surface plots showing the parametric effects on temperature for (a-c) MQL, (d-f) NF-MQL lubrication environment

In the machining zone, nanoparticle-based mist produces a stable thin layer which causes excellent performance than the mineral oils. When water-based nano-fluids are imposed on the machining zone, water particles evaporate rapidly generating a film of nanoparticles [9]. This thin layer enhances the lubrication effect through tribo-film feature. Moreover, shearing heat is removed from the machining zone through the high-pressure mist-air mixture and temperature is dissipated through rapid fluid evaporation. Deionized water has a specific heat of 4.2 kJ/kg K at 20°C which is almost two times than the canola oil (2.4 kJ/kg K). Therefore, dehydration of the water droplets of the H_2O-Cu produces (Fig. 6 as inspired by [48]) an excellent cooling effect as compared to biodegradable oils [31].

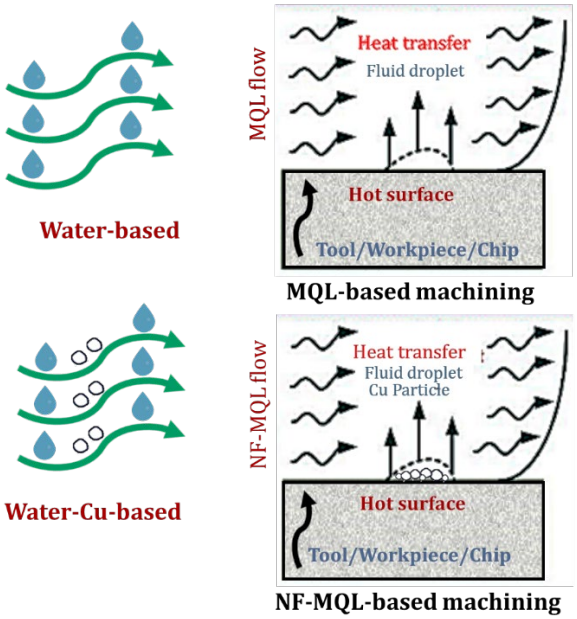

Figure 6. Mechanism of heat transfer in MQL and NF-MQL systems.

3.1.3 Response surface plots for material removal rate

Fig. 7a and Fig. 7d represent the effects of F_{IR} and D_{OC} on material removal rate. It is clear from 3D response surface plots that MRR is more affected by D_{OC} than Fl_R for both the environments. The effects of S_P and

D_{OC} on material removal rate for MQL and NF-MQL have been described using Fig. 7b and Fig. 7e, respectively. It can be identified that for both environments. D_{OC} has more effect on material removal rate as compared to S_P which has approximately no effect. Moreover, the maximum material removal rate is attained at a high level of D_{OC}. The impacts of D_{OC} and F_R on material removal rate for the MQL lubrication environment are shown in Fig. 7c, It can be noticed that MRR increases with increment in D_{OC} and F_R. Similar behaviour for NF-MQL lubrication has been observed (Fig. 7f). Increase in material removal rate which directs the productivity is always desired. Therefore, MQL and NF-MQL are admirable options [37]. As the S_P rises then MRR also increases, the machine tool consumed high energy which ultimately forces the system to consume more energy. When S_P reaches up to a certain high level, frictional heat produced at the interface of tool-chip also rises and sufficient heat passes in the tool-workpiece surface causing the thermal softening [45]. Plenty of energy is consumed to eradicate the hard grains of nickel alloys during the machining of IN718. The increasing feed rises the cutting energy because of additional resistance of the shearing region at the workpiece material. Under the nanofluids machining, the variation in cutting energy can be accredited to the decline in tool wear because of the better lubri-cooling effect that barred thermal softening of the tool. It can be concomitant with the excellent stability and higher thermal conductivity of Cu-based nanofluid [31] than simple MQL [22]. Finally dispersed nanofluid infiltrates to cutting region acted as barriers to reduce the persuaded rubbing of the tool on the surface of the workpiece, developing a tribo-film (nano additive plowing) effect as discussed earlier [49]. Therefore at higher levels of F_R in contrast with S_P, tribo-film and ball-bearing effect reduced built-up edge formation which eventually lower the friction and energy consumption.

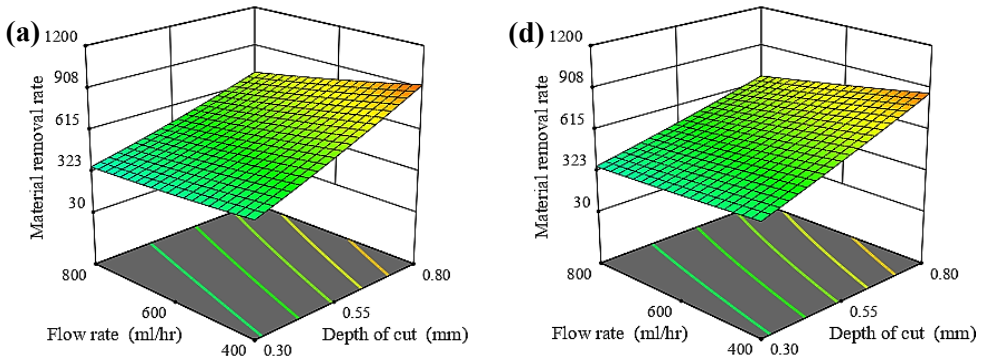

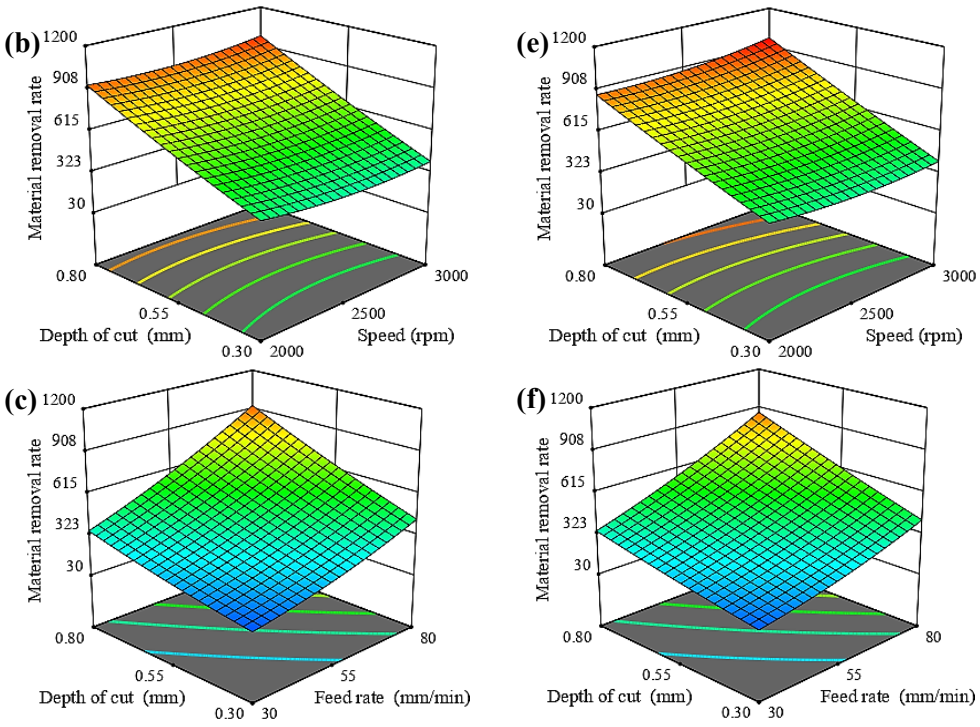

Figure 7. Response surface plots showing the parametric effects on material removal rate for (a-c) MQL, (d-f) NF-MQL lubrication environment

3.1.4 Response surface plots for power consumption

Flood machining utilizes more power than other cutting fluid approaches, for the large cutting length. The motor is essential to run the pump for circulation of emulsion. It enhances the need for power consumption for flood machining. Fig. 8a and Fig. 8d demonstrate the effects of S_P and F_R on power for MQL and NF-MQL lubrication environments respectively. The comparative analysis between both environments shows similar effects of varying S_P and F_R on power. Power increases with addition in S_P and F_R. It is valuable to note that minimum power has been achieved for NF-MQL lubrication. The effects of D_{OC} and SP on power have been presented for both conditions in Fig. 8b and Fig. 8e. The figures indicate that power is minimum at low levels of D_{OC} and S_P and vice versa. Additionally, the effect of D_{OC} on power is very large than S_P. Fig. 8c and Fig. 8f depict the effects of Fl_R and S_P on power under both conditions. For both environments, it is evident that power increases with increment in S_P and inverse with Fl_R. Furthermore, S_P has more effect on power as compared to Fl_R. A similar observation is made in the literature [50].

Fig. 2(b) depicts the nanofluid supply during the NF-MQL milling. Through the pressurized air, nanofluid is atomized in the nozzle and changed into a fine mist. The velocity of mist is higher than the rotational speed of the tool, so it can pass in the shearing region generate the gap among the tool-workpiece to lubricate the cutting region. In the case of water-based nanofluid mist, water droplets evaporated rapidly and nanoparticles deposit on the surface of workpiece and tool [7]. The presence of nanoparticles in

cutting region origin the tribo-film formation that improves the lubrication in the shearing zone which ultimately reduce the frictional shear stress and decline the tangential cutting force [26].

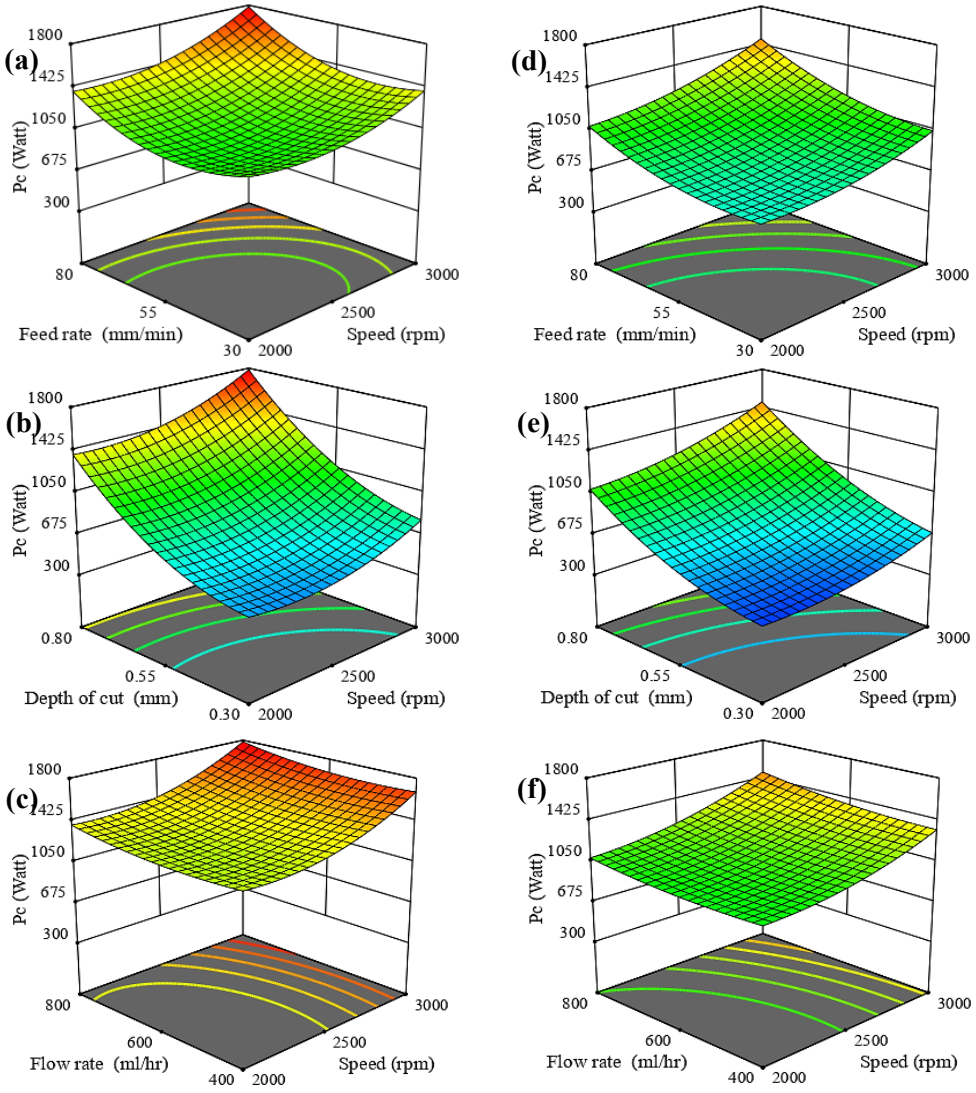

Figure 8. Response surface plots showing the parametric effects on power for (a-c) MQL (d-f) NF-MQL lubrication environment

To sum up, introducing nano lubrication gives lesser cutting force and power consumption. This is primarily ascribed to the presence of nanoparticles in the fluid that provides the support in reducing friction at the tool-workpiece interaction area. Moreover, these nanoparticles come in direct contact with tool and workpiece which work as a combination of rolling and sliding bearings at the tool chip zone and results in a reduction on the coefficient of friction deliberately. Thus, a lower cutting force is attained in the nano-lubrication system when comparing to MQL. It leads to the decline of specific energy and power needed during the process [51].

3.2 Surface morphological analysis

SEM images of MQL and NF-MQL milling samples have been taken for different parametric conditions: Fig. 9 (a, d) for S_P 2500 rpm, F_R 55 mm/min, D_{OC} 0.05 mm, F_{lR} 600 ml/hr**;** Fig. 9(b, e) for S_P 1500 rpm, F_R 55 mm/min, D_{OC} 0.55 mm, Fl_R 600 ml/hr, and Fig. 9(c, f) for S_P 3500 rpm, F_R 55 mm/min, D_{OC} 0.55 mm, Fl_R 600 ml/hr. In the machining of IN718, there are surface defects such as scratches, groove, cracks, feed marks. These defects have adverse effects on the machined surface and further leads to the inferior surface quality (Fig. 9(a)). Under the action of comparative thermal load in MQL, the surface becomes more viscous and plastic flow occurs, and scratches and feed marks are formed on the milled surface (Fig. 9(a,b,c)). It is evident from the Fig. 9 that medium speed has resulted in the lowest SR 0.04 μm for NF-MQL and 0.06 μm in case of MQL milling. The worst results of SR 0.24 μm and 0.29 μm has been observed for the lowest speed for both conditions because at higher depth of cut thick feed marks formed at the machined surface. These thick marks show the occurrence of some discontinuity like plucking along the machined surface. Nanofluids reduces the feed marks on the milled surfaces, which is shown in the SEM texture images. Smearing, grooves, and scratches are less in the NF-MQL conditions in comparison to other lubrication condition.

It is reported in the literature that the shape of the discrete nanoparticles is virtually spherical and size is in the nanometric range [17]. Nanoparticles can effortlessly be infiltrated into the interaction surfaces between the tool-workpiece and chip. In addition, comparatively smooth surface in terms of magnitude of feed marks is observed through NF-MQL (see Fig. 9 (d,e,f)). These nanoparticles act as a third body in the cutting region, which can abide by the normal tool cutting load and split the interaction surfaces. Moreover, these spherical nanoparticles can roll between the interaction surfaces like the ball bearing during the milling which enable a change on the pure sliding friction among the interaction surfaces into the mixed friction (rolling and sliding). Thus, the friction and tangential cutting force reduced in the NF-MQL milling [51]. Elastic and plastic deformation occurs on the rubbing interface as the interaction surfaces slide against each other in the milling process. As it is established that under comparatively lower normal load, elastic deformation for the surface severities is prevailing (phenomena shown in Fig. 10). While the plastic deformation preponderates under relatively higher normal load. Moreover, we speculate that the friction enhanced with increment in applied load due to the plastic deformation layer that arises on the sliding surface and numerous dislocations are formed. When the concentration of nanofluid is high in case of high flow rate (Fl_R), then it is obvious that the number of nanoparticles will be high in the cutting region [8]. It results in a normal load of single nanoparticle applied by the normal cutting force for the low concentration is higher than the higher concentration of nanofluids. Moreover, the plastic deformation of

the rubbing surfaces is slighter in case of high flow rate than the lower. Hence, NF-MQL milling with high flow rate shows excellent friction reducing ability which results in a decrease in surface roughness (SR).

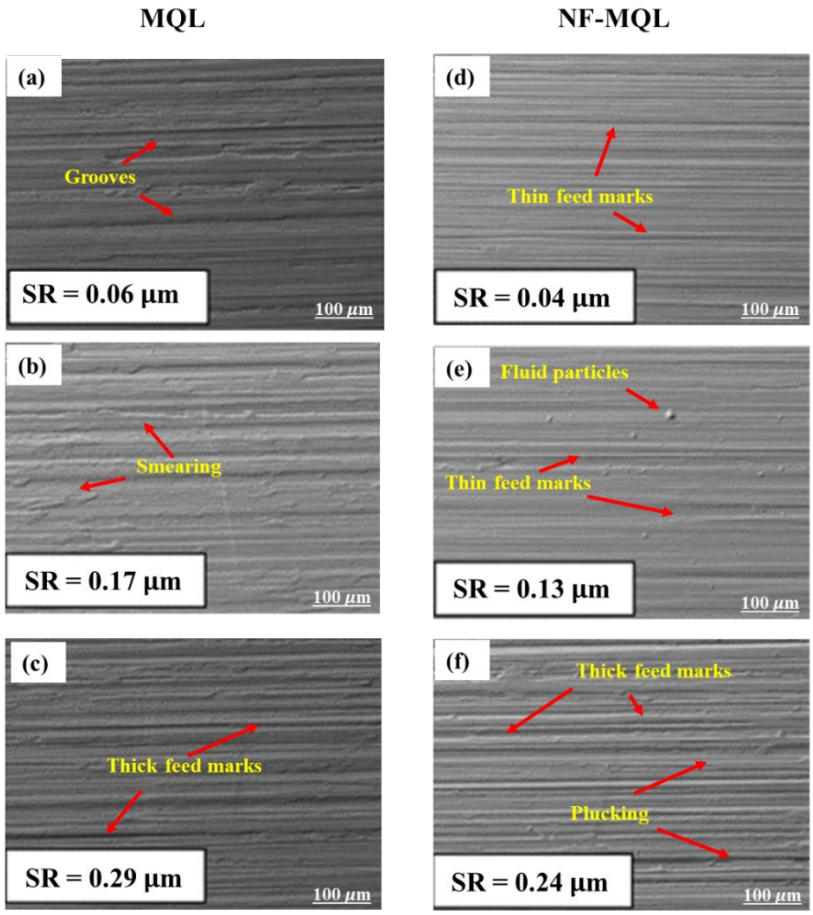

Figure 9. SEM-based surface morphological analysis (a, d) S_P 2500 rpm, F_R 55 mm/min, D_{OC} 0.05 mm, Fl_R 600 ml/hr, (b, e) S_P 1500 rpm, F_R 55 mm/min, D_{OC} 0.55 mm, Fl_R 600 ml/hr, and (c, f) S_P 3500 rpm, F_R 55 mm/min, D_{OC} 0.55 mm, Fl_R 600 ml/hr.

The Fig. 11 reveals that with the increase in speed, the surface characteristics are favorable in both lubrication environments. The adequate balance of speed with other process parameters influences the results significantly. The speed of 2500 rpm results in better surface roughness in MQL as well as NF-MQL environment as displayed in Fig. 11(a, d), whereas, highest speed 3000 rpm leads towards ineffectiveness of the lubrication techniques. This is because that the nanofluids cannot perform the required action on the surface due to mismatch between the flow rate and spindle rotation speed. Therefore, comparatively higher irregularities are evident in Fig. 11(b, e). However, lower speed also does not compensate for the required action ability of minimum quantity lubrication. At lower speed 2000 rpm, remarkably higher surface roughness is obtained as shown in Fig. 11(c, f). The interactions among the cutting tool, chip and workpiece are known as interfaces which can be categorized such as chip-tool interface, tool-workpiece

interface and chip-workpiece interface. These interfaces behave as friction factors; cutting tool-workpiece involve sliding friction, chip removal and plowing [42]. Mainly three friction mechanisms (plowing, adhesion and plastic deformation) may exist in machining.

Rubbing surfaces can cause adhesion due to the repetitive formation and splitting of atomic bonding and it has an impact on the surface roughness. Additives are embedded in machining process to handle the adhesion. Plastic deformation leads to the emergence of motion resistance for rubbing surfaces and it is imperative for friction and wear [52]. Therefore, plastic deformation has a substantial impact on the surface roughness. However, plowing that is close to burnishing mechanism, and is observable while applying the scratch on the machined surface has a direct effect on the surface roughness [6]. The friction is pigeonholed by high tribological stress in the machining process. During the machining process, three frictional mechanisms (plowing, adhesion and plastic deformation) can be reduced by the improvement of lubrication effect and by the abrasive nanoparticles [51]. Surface roughness reduces also due to the formation of excessive chips through micro-cutting action by sharp abrasive nano-particles.

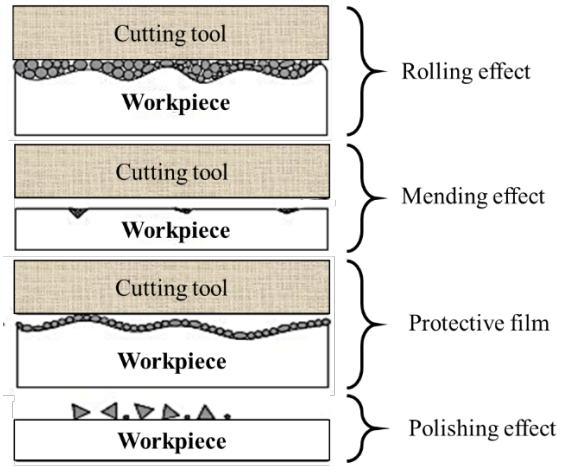

Figure 10. Tribological mechanisms at surface during NF-MQL.

The mechanism behind tribological aspects introduced through nanofluid lubrication is confirmed by reduced friction and wear patterns. The improved surface features enhance the properties for tribological applications. The MQL-based mechanism produces messiest, scallops and deeper scratches as compared to surface produced by NF-MQL that shows smooth features with very few spalls and pits. The physical science behind this phenomenon is evident in Fig. 10. The nano-fluids improves surface through rolling action which acts as grinding process to improve the surface irregularities. The plastic deformation on the layer is controlled through friction-reduction properties of nanofluid, and it also supports through mending action to repair the surface from forming microcracks. These microcracks, if surface does not have nanofluid protective layer, propagate under the action of continuous loading ultimately fragmenting

and damaging the surface [53]. As evident in Fig. 9, nanofluid improves resistance against micro-abrasion and adhesive wear.

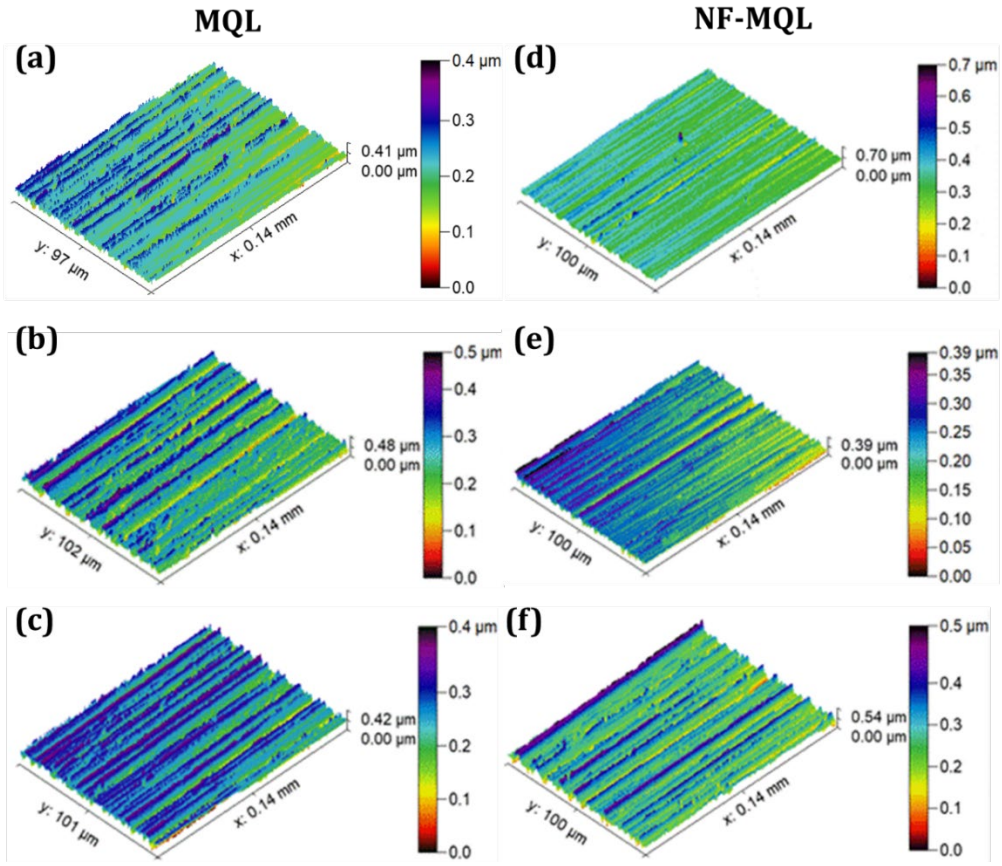

Figure 11. 3D-surface topography IN718 processed samples under lubrication conditions: (a, d) S_P 2500 rpm, (b, e) S_P 3000 rpm, and (c, f) S_P 2000 rpm.

The wear mechanism of machining tool is strappingly reliant on machining parameters, tool type [54], workpiece and lubrication conditions [23]. Tool wear also is responsible for more energy consumption by the cutting tool in the machining of difficult-to-cut materials [6]. Cu nano additive-assisted NF-MQL worked as a barrier to decrease the rubbing of cutting edge on the surface of the workpiece and withstand for a longer duration on the surface of the tool as shown in Fig. 12. The catastrophic failure of tool happened during dry conditions which was a baseline for improvement in term of tool life, as Fig. 12(Dry) shows the physical evidence. During dry cutting, the forces become high and cause high friction [45]. MQL based process improved tool life significantly than the dry conditions. The phenomenon of adhesion and abrasion can be observed in Fig. 12(MQL). Actually, at high feed and cutting speed, the temperature became high at the tool-chip interface. Due to high temperature, a fine mist of MQL can evaporated rapidly and in the mean time allows enough flow to disperse the heat from the machining region. A vapour layer

between tool-workpiece contact is generated by the evaporating mist named as Leiden frost effect [2]. The formation of this vapour layer delays the heat-transferring efficiency for that additional lead to chip adhesion and tool wear [50]. However, NF-MQL assisted machining improved the tool life the most as evident from Fig. 12(NF-MQL). This is because of the rolling action of the Cu-based nanoparticles.

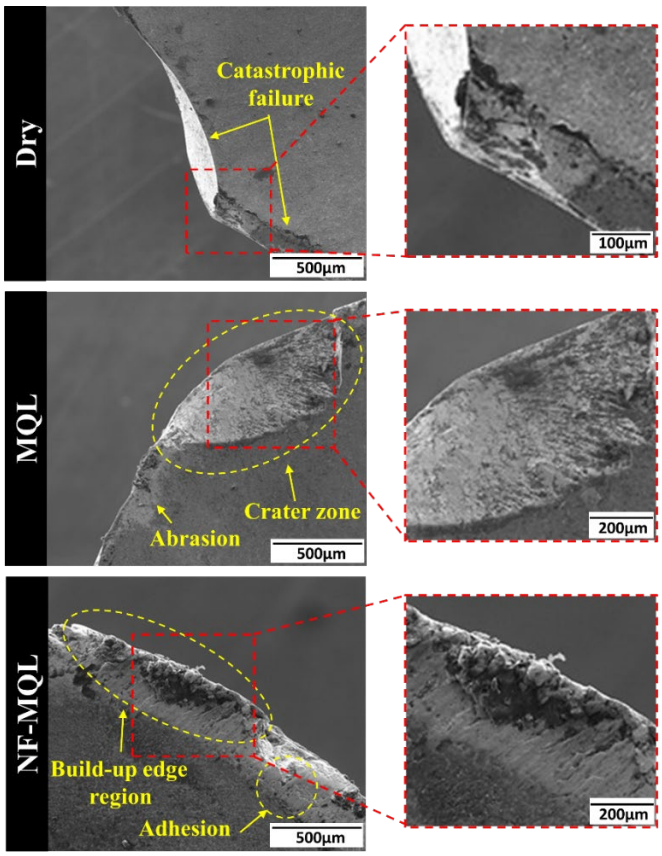

Figure 12. SEM images for tool flank wear analysis under various conditions: Dry, MQL and NF-MQL milling

3.3 Parametric significance analysis

The statistical analysis helps to quantify the effects of process variants to better understand the system dynamics as well as to optimize the overall performance. Therefore, the significance of statistical analyses can not be overruled. The understanding of tribological aspects without quantifying it adequately can lead towards neglection of an important phenomenon which can harm service quality. The research aims to investigate surface characteristics of aerospace alloy processed through face milling under the action of water-based MQL and Cu-water based NF-MQL. This methodology will lead towards reducing residual stresses and improved surface characteristics of IN718 which is primarily used in aero engines.

ANOVA results revealed that the main effects of D_{OC} and quadratic effects of S_P^2, F_R^2 and D_{OC}^2 were the crucial model terms related to surface roughness for milling under MQL lubrication conditions (Table 3). Alike effects

were observed noteworthy for NF-MQL condition. The main and quadratic effects that contribute significantly in temperature under both lubrication environments include D_{OC}, S_P^2, F_R^2 and D_{OC}^2.

Table 3. ANOVA tables for SR and temperature under both (MQL and NF-MQL) lubrication environments

Surface roughness (MQL)						Surface roughness (NF-MQL)					
Source	**SS**	**df**	**MS**	**F value**	**p-value**	**Source**	**SS**	**df**	**MS**	**F value**	**p-value**
Model	0.100	4	0.026	58.73	< 0.0001	Model	0.0710	4	0.0177	51.93	< 0.0001
D_{OC}	0.062	1	0.062	142.65	< 0.0001	D_{OC}	0.0459	1	0.0459	34.45	< 0.0001
S_P^2	0.012	1	0.012	27.63	< 0.0001	S_P^2	0.0075	1	0.0074	21.88	< 0.0001
F_R^2	0.029	1	0.029	65.80	< 0.0001	F_R^2	0.0176	1	0.0176	51.58	< 0.0001
D_{OC}^2	0.008	1	0.008	18.53	0.0002	D_{OC}^2	0.0054	1	0.0053	15.69	0.0005
Residual	0.011	25	0.0004			Residual	0.0085	25	0.0003		
Lack of fit	0.009	20	0.0005	2.83	0.1263	Lack of fit	0.0077	20	0.0004	2.17	0.1998
Pure error	0.0008	5	0.0002			Pure error	0.0009	5	0.0002		
Cor total	0.11	29				Cor total	0.0795	29			
Std. Dev.	0.021		R^2		0.9038	Std. Dev.	0.018		R^2		0.8926
Mean	0.17		Adjusted R^2		0.8884	Mean	0.13		Adjusted R^2		0.8754
C.V. %	12.27		Predicted R^2		0.8354	C.V. %	13.59		Predicted R^2		0.8029
Press	0.019		Adequate precision		23.887	Press	0.016		Adequate precision		23.190
Temperature (MQL)						**Temperature (NF-MQL)**					
Source	**SS**	**df**	**MS**	**F value**	**p-value**	**Source**	**SS**	**df**	**MF**	**F value**	**p-value**
Model	58709.9	4	14677.48	61.39	< 0.0001	Model	37212.2	9	4134.6	21.27	< 0.0001
D_{OC}	30602.0	1	30602.04	128.00	< 0.0001	S_P	925.04	1	925.04	4.76	0.0412
S_P^2	5245.7	1	5245.73	21.94	< 0.0001	F_R	1457.04	1	1457.0	7.49	0.0127
F_R^2	13321.9	1	13321.98	55.72	< 0.0001	D_{OC}	11223.38	1	11223.3	57.75	< 0.0001
D_{OC}^2	15876.9	1	15876.98	66.41	< 0.0001	Fl_R	1276.04	1	1276.04	6.56	0.0186
Residual	5977.0	25	239.08			$F_R \times D_{OC}$	1278.06	1	1278.06	6.57	0.0185
Lack of fit	5557.5	20	277.88	3.31	0.0941	$F_R \times Fl_R$	3052.56	1	3052.56	15.71	0.0008
						S_P^2	5314.39	1	5314.39	27.35	< 0.0001
Pure error	419.50	5	83.90			F_R^2	13431.27	1	13431.2	69.11	< 0.0001
Cor total	64686.9	29				D_{OC}^2	2885.64	1	2885.6	14.85	0.0010
Std. Dev.	15.46		R^2		0.9076	Residual	3886.693	20	194.33		
Mean	147.03		Adjusted R^2		0.8928	Lack of fit	3523.86	15	234.92	3.24	0.1000
C.V. %	10.52		Predicted R^2		0.8075	Pure error	362.8333	5	72.56		
Press	12450.88		Adequate precision		26.403	Cor total	41098.97	29			
						Std. Dev.	13.94		R^2		0.9054
						Mean	123.37		Adjusted R^2		0.8629
						C.V. %	11.30		Predicted R^2		0.7046
						Press	12138.76		Adequate precision		14.633

For NF-MQL milling additional main effects of S_P, F_R and Fl_R; and interaction effects of ($F_R \times D_{OC}$), ($F_R \times Fl_R$) was found significant (Table 3). ANOVA results highlighted that main effects of F_R and D_{OC}; interaction effects of ($F_R \times D_{OC}$) and ($D_{OC} \times Fl_R$) and quadratic effects of S_P^2 and F_R^2 are the significant model's terms associated with material removal rate for milling under both lubrication environments (Table 4). Main and quadratic effects of S_P, F_R, D_{OC}, S_P^2, F_R^2 and D_{OC}^2 were the significant model's terms related power for milling under both the lubrication environment as highlighted by ANOVA results (Table 4).

Table 4. ANOVA tables for MRR and P_C under both (MQL and NF-MQL) lubrication environments

Material removal rate (MQL)						Material removal rate (NF-MQL)					
Source	**SS**	**df**	**MS**	**F value**	**p-value**	**Source**	**SS**	**df**	**MS**	**F value**	**p-value**
Model	$1.74\times10^{+6}$	6	289313.5	49.93	< 0.0001	Model	1630817.5	6	271802.92	52.78	< 0.0001
F_R	$9.26\times10^{+5}$	1	926301	159.87	< 0.0001	F_R	875162.04	1	875162.04	169.93	< 0.0001
D_{OC}	$6.62\times10^{+5}$	1	661676	114.20	< 0.0001	D_{OC}	640593.38	1	640593.38	124.39	< 0.0001
$F_R \times D_{OC}$	70623.06	1	70623.06	12.19	0.0020	$F_R \times D_{OC}$	54172.56	1	54172.56	10.52	0.0036
$D_{OC} \times Fl_R$	23180.06	1	23180.06	4.00	0.0574	$D_{OC} \times Fl_R$	13514.06	1	13514.06	2.62	0.1189
S_P^2	34055.63	1	34055.63	5.88	0.0236	S_P^2	30058.89	1	30058.89	5.84	0.0240
F_R^2	25988.13	1	25988.13	4.48	0.0452	F_R^2	22512.50	1	22512.50	4.37	0.0478
Residual	$1.33\times10^{+5}$	23	5794.172			Residual	118449.92	23	5150.00		
Lack of fit	$1.17\times10^{+5}$	18	6515.841	2.04	0.2210	Lack of Fit	112374.42	18	6243.02	5.14	0.0394
Pure error	15980.83	5	3196.167			Pure Error	6075.50	5	1215.10		
Cor total	$1.87\times10^{+6}$	29				Cor Total	1749267.4	29			
Std. Dev.	76.12		R^2		0.9287	Std. Dev.	71.76		R^2		0.9323
Mean	412.8		Adjusted R^2		0.9101	Mean	409.53		Adjusted R^2		0.9146
C.V. %	18.44		Predicted R^2		0.8731	C.V. %	17.52		Predicted R^2		0.8722
Press	237148.8		Adequate precision		23.495	PRESS	223476.28		Adequate precision		23.914
Power (MQL)						**Power (NF-MQL)**					
Source	**SS**	**df**	**MS**	**F value**	**p-value**	**Source**	**SS**	**df**	**MS**	**F value**	**p-value**
Model	6074102	6	1012350	33.78	< 0.0001	Model	2802380.6	6	467063.44	26.12	< 0.0001
S_P	347282	1	347282	11.59	0.0024	S_P	256060.04	1	256060.04	14.32	0.0010
F_R	211125	1	211125	7.04	0.0142	F_R	232657.04	1	232657.04	13.01	0.0015
D_{OC}	3767545	1	3767545	125.70	< 0.0001	D_{OC}	1698676.0	1	1698676.0	94.99	< 0.0001
S_P^2	401581.6	1	401581.6	13.40	0.0013	S_P^2	146197.88	1	146197.88	8.18	0.0089
F_R^2	921203.6	1	921203.6	30.74	< 0.0001	F_R^2	254079.38	1	254079.38	14.21	0.0010
D_{OC}^2	835678.1	1	835678.1	27.88	< 0.0001	D_{OC}^2	358380.00	1	358380.00	20.04	0.0002
Residual	689352.8	23	29971.86			Residual	411286.34	23	17882.01		
Lack of fit	619740	18	34430	2.47	0.1606	Lack of Fit	354863.00	18	19714.61	1.75	0.2797
Pure error	69612.83	5	13922.57			Pure Error	56423.33	5	11284.67		
Cor total	6763455	29				Cor Total	3213666.9	29			
Std. Dev.	173.1238		R^2		0.8980	Std. Dev.	133.72		R^2		0.8720
Mean	921.6333		Adjusted R^2		0.8714	Mean	749.03		Adjusted R^2		0.8386
C.V. %	18.78446		Predicted R^2		0.7240	C.V. %	17.85		Predicted R^2		0.7435
Press	1866213		Adequate precision		19.369	PRESS	824315.86		Adequate precisio		18.140

3.4 Mathematical modelling and predictive analysis

3.4.1 Surface roughness

For both the MQL and NF-MQL milling environments, ANOVA summary suggests that the quadratic relationship is the best fit model. ANOVA results consisting of vital model terms with adequacy measures R^2, adjusted R^2 and predicted R^2 for both the lubrication environments have been presented in Table 3. The results indicate the models are significant as the p-values are less than 0.05. Adequacy measures R^2, adjusted R^2 and predicted R^2 are near to unity which indicates the acceptability of the developed models. Empirical models for the prediction of surface roughness under MQL and NF-MQL lubrication environments have been presented in Eq. 3 and Eq. 4, respectively.

$$SR_{MQL} = 0.11 + 0.051 \times D_{OC} + 0.021 \times S_P^2 + 0.032 \times F_R^2 + 0.017 \times D_{OC}^2 \quad (3)$$

$$SR_{NF-MQL} = 0.092 + 0.044 \times D_{OC} + 0.016 \times S_P^2 + 0.025 \times F_R^2 + 0.014 \times D_{OC}^2 \quad (4)$$

3.4.2 Temperature

ANOVA results provided in Table 3 highlight that the models are considerable. Empirical models developed to ensure predictability of the temperature for both MQL and NF-MQL lubrication are presented in Eq. 5 and Eq. 6, respectively.

$$T_{MQL} = 99.58 + 35.71 \times D_{OC} + 13.69 \times S_P^2 + 21.81 \times F_R^2 + 23.81 \times D_{OC}^2 \quad (5)$$

$$T_{NF-MQL} = 86.70 + 6.21 \times S_P + 7.79 \times F_R + 21.62 \times D_{OC} - 7.29 \times D_{OC} \times Fl_R + 8.94 \times F_R \times D_{OC} + 13.81 \times F_R \times Fl_R + 13.78 \times S_P^2 + 21.90 \times F_R^2 + 10.15 \times D_{OC}^2 \quad (6)$$

3.4.3 Material removal rate

For both the MQL and NF-MQL milling environments, ANOVA summary suggests the quadratic relationship is the best fit model in case of material removal rate. ANOVA results consisting of significant model terms with R^2, adjusted R^2 and predicted R^2 for both the lubrication environments have been given in Table 4. The empirical models for the prediction of the material removal rate under MQL and NF-MQL lubrication conditions have been presented using Eq. 7 and Eq. 8, respectively.

$$MRR_{MQL} = 360.94 + 196.46 \times F_R + 166.04 \times D_{OC} - 38.06 \times D_{OC} \times Fl_R + 66.44 \times F_R \times D_{OC} + 34.60 \times S_P^2 + 30.23 \times F_R^2 \quad (7)$$

$$MRR_{NF-MQL} = 361.02 + 190.96 \times F_R + 163.37 \times D_{OC} - 29.06 \times D_{OC} \times Fl_R + 58.19 \times F_R \times D_{OC} + 32.51 \times S_P^2 + 28.13 \times F_R^2 \quad (8)$$

3.4.4 Power

ANOVA results containing significant model terms with R^2, adjusted R^2 and predicted R^2 are provided in Table 4. The result indicates that models are significant. The values of adequacy measures R^2, adjusted R^2 and predicted R^2 near to unity indicate the adequacy models. Empirical models for the prediction of the temperature under MQL and NF-MQL lubrication have been provided in Eq. 9 and Eq. 10, respectively.

$$Power_{MQL} = 542.51 + 120.29 \times S_P + 93.79 \times F_R + 396.21 \times D_{OC} + 199.76 \times S_P^2 + 181.38 \times F_R^2 + 172.76 \times D_{OC}^2 \quad (9)$$

$$Power_{NF-MQL} = 524.51 + 103.29 \times S_P + 98.46 \times F_R + 266.04 \times D_{OC} + 72.26 \times S_P^2 + 95.26 \times F_R^2 + 113.13 \times D_{OC}^2 \quad (10)$$

3.4.5 Validation of the empirical models

To validate the established empirical models, six confirmation trials were conducted for both the environments. The values of process variables selected for these experiments were different from those used for models development [55]. The difference between predicted and actual values obtained from the confirmation experiments has been expressed in the form of percentage error using Eq. 11 [56]. The validation results for MQL and NF-MQL milling have been given in Table 5. The results depict that the experimental and predicted values are closer to each other with a maximum error of 4.7%. It can be

determined from the findings that the empirical models for both lubrication environments have the capability for the prediction of responses with accuracy.

$$\text{Percentage error} = \left|\frac{\text{actual value} - \text{predicted value}}{\text{predicted value}}\right| \times 100 \quad (11)$$

Table 5. Validation results for MQL and NF-MQL milling conditions

Process parameter						Observed performance measures							
						SR		**T**		**MRR**		**P_C**	
Run	**S_P**	**D_{OC}**	**F_R**	**Fl_R**		MQL	NF-MQL	MQL	NF-MQL	MQL	NF-MQL	MQL	NF-MQL
1	2100	0.40	40	450	Experimental	0.119	0.087	102	100	195	195	468	425
					Predicted	0.121	0.090	100	96	188	195	448	445
					% Error	1.6	3.3	1.2	4	3.8	0	4.2	4.4
2	2600	0.65	65	650	Experimental	0.136	0.115	114	97	515	516	746	688
					Predicted	0.140	0.116	117	106	494	514	778	707
					% Error	2.8	4.3	2.5	3.9	4.4	2.9	4.5	2.7
3	2900	0.75	75	750	Experimental	0.208	0.157	175	145	732	733	812	1216
					Predicted	0.200	0.160	171	149	706	713	778	1190
					% Error	3.8	2.5	1.8	2.6	3.8	2.9	4.1	2.2
4	2200	0.50	35	550	Experimental	0.136	0.104	107	90	186	209	507	420
					Predicted	0.130	0.100	105	94	189	201	480	435
					% Error	4.4	3.8	1.9	4.2	1.7	4.3	4	3.6
5	2800	0.35	65	650	Experimental	0.100	0.080	90	89	303	310	462	470
					Predicted	0.098	0.076	92	85	291	298	445.2	458
					% Error	2	5	2.7	4.4	4.3	3.8	3.6	2.8
6	2400	0.45	75	750	Experimental	0.130	0.102	104	104	392	413	545	500
					Predicted	0.126	0.099	101	99	402	409	532	515
					% Error	**3**	**2.9**	**2.5**	**4.7**	**2.5**	**1**	**2.3**	**2.9**

3.5 Machinability comparative analysis

The discussion in the preceding sections noticeably demonstrates that NF-MQL reduces surface roughness, temperature and power consumption. To further elaborate on the effectiveness of NF-MQL, comparison between both lubrication environments for all performance measures has been provided in Fig. 13. These figures have been drawn from the design space. From the Fig. 13(a-d), it is evident that nano-particles based MQL milling provides better results with an average percentage reduction of 20.1%, 14.7% and 13.3% in surface roughness, temperature and power respectively. Whereas, a very minute difference between the two environments has been observed for material removal rate.

The MQL improves temperature control, cutting force distribution as well as reduces friction. This leads to enhancing machinability aspects such as surface roughness, material removal rate, tool wear rate in comparison to conventional lubrication methods [50]. Moreover, the nano-particles helps to improve thermal conduction, evident from results discussed earlier and induces tribological features at the point of tool-workpiece interaction [57]. An additional polishing characteristic is added to the process with the help of nano-fluids. However, it does not significantly improve material removal as compared to MQL (see

Fig. 13(c)). This is because it mainly helps to achieve higher surface integrity and quality (see Fig. 13(a, b)). The addition of the material removal rate as the performance index is due to the goal to explore all machinability aspects under sustainable lubrication technique [37].

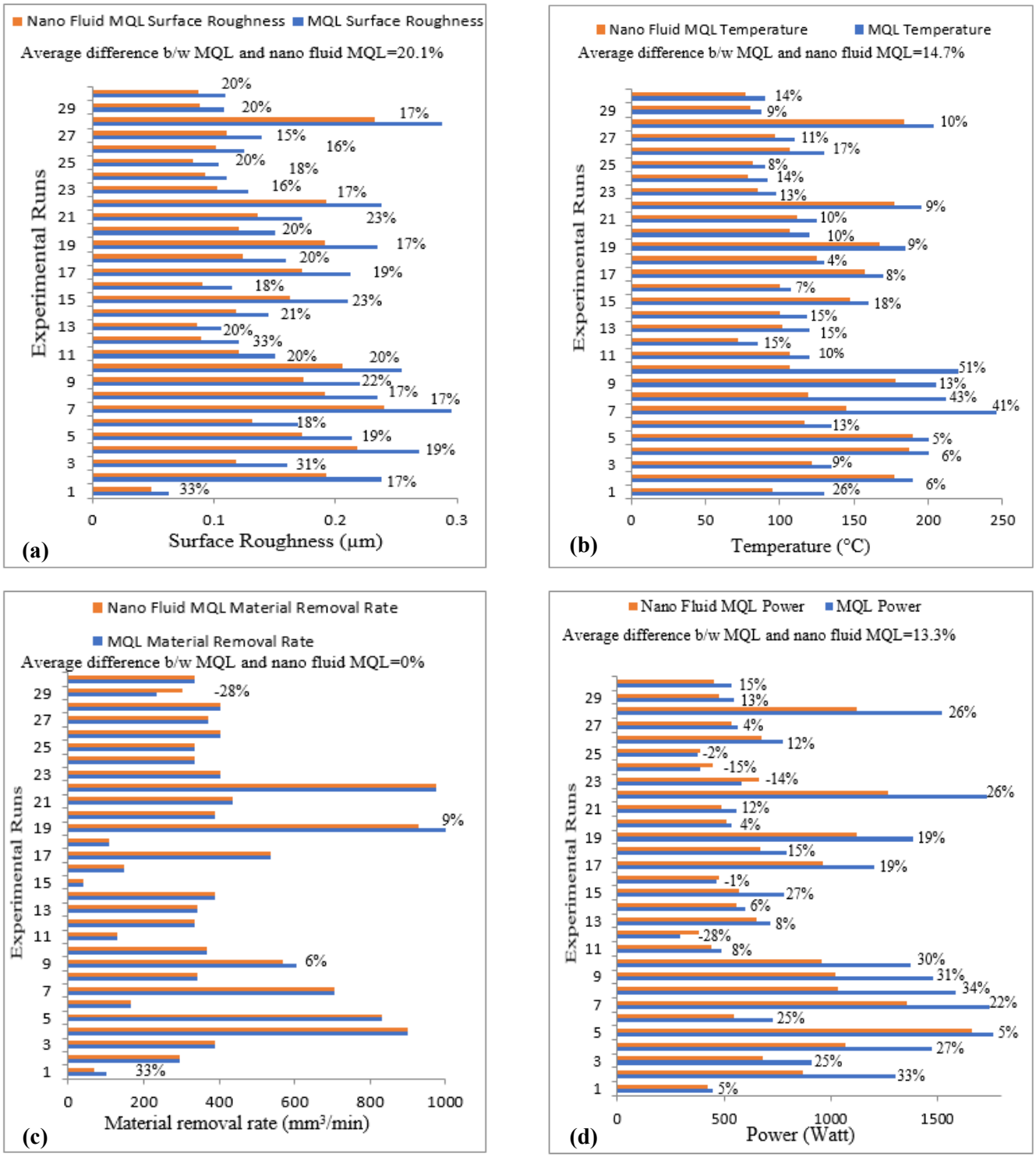

Figure 13. Comparison of performance measures for MQL and NF-MQL environments

3.6 Sustainability-based empirical analysis

This research aims to accomplish sustainable production [51] which can be obtained by making superior quality parts with a high production rate and less power consumption [50]. The performance measures directly associated with these three sustainable production attributes include surface roughness, material removal rate and power consumption. Furthermore, temperature indirectly influences sustainable production as it has a significant impact on surface roughness, material removal rate and power consumption. Thus, all the responses desire to be articulated in the single sustainability goal function as given in Eq. 12 to achieve sustainability.

$$\text{Sustainability} = \begin{cases} \text{Minimize Surface Roughness} \\ \text{Minimize Temperature} \\ \text{Maximize Material Removal Rate} \\ \text{Minimize Power Consumption} \end{cases} \tag{12}$$

Fig. 14 demonstrates the summarized findings of the detailed assessment of 3D response surface plots. It expresses the impact of the process variables on output measures. In figure, two functions; (i) 'As-is function' (achieved function), and (ii) 'To-be function' (desired sustainability function) have been employed. The achieved impacts of increasing parameters on performance measures have been obtained by As-is function. While 'To-be function', describes the benchmarked desired sustainability function as given in Eq. 12. To-be function can be attained by maximizing the MRR while minimizing the temperature, SR and power, simultaneously. Certainty, this 'To-be function' cannot be attained by increasing any of the process parameters. For instance, by increasing feed rate, all four performance responses (surface roughness, temperature, material removal rate and power) increases.

The above discussions conclude that sustainable objective function cannot be attained directly. Multi-objective optimization based on desirability function has been carried out to overcome this limitation. The purpose of multi-objective optimization is to incorporate the impacts of multiple performance measures using mathematical transformation function into a single desirability value. This single desirability value has been achieved in two phases; (i) desirability identification (di), and (ii) combined desirability geometric mean (CDGM) formulation. In di phase, each performance measure (Yi) was normalized to obtain desirability value (di) has range $0 \leq di \leq 1$, where 0 specifies the most unwanted value and 1 represents the most wanted value. Once the desirability of all the individual performance measures has been attained, they were pooled into a single value using CDGM in the second phase. The desirability functions for maximizing MRR, while minimizing surface roughness, temperature, power consumption and CDGM have been given in Eq. 13, Eq. 14 and Eq. 15, respectively [58].

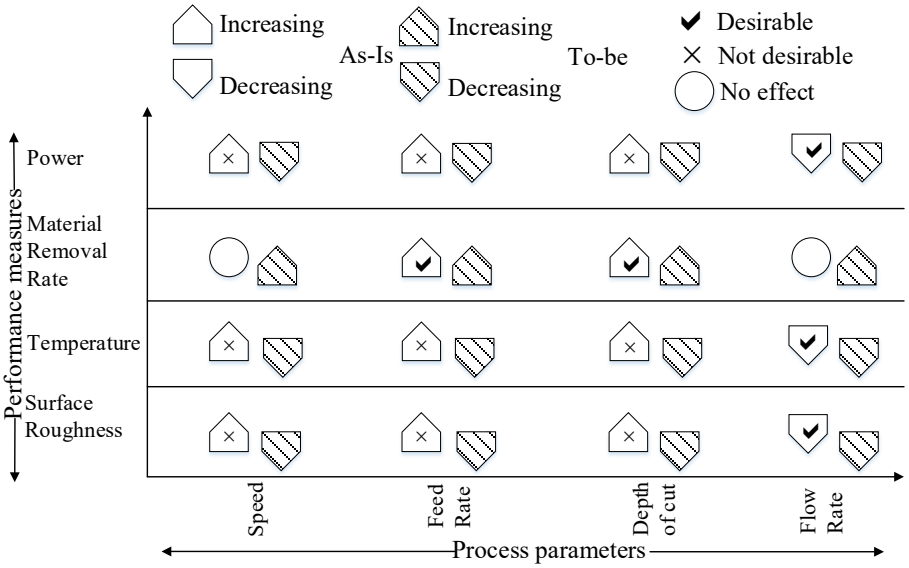

Notation: signifies increasing function and signifies decreasing function

Figure 14. As-is and To-be sustainability function of the performance measures

$$d_i = \begin{cases} 0, Y_i \le L_i \\ \left(\frac{H_i - Y_i}{H_i - L_i}\right)^w, \; L_i < Y_i < H_i \\ 1, Y_i \le H_i \end{cases} \quad (13)$$

$$d_i = \begin{cases} 0, Y_i \le L_i \\ \left(\frac{H_i - Y_i}{H_i - L_i}\right)^w, L_i < Y_i < H_i \\ 1, Y_i \ge H_i \end{cases} \quad (14)$$

$$CDGM = (d1 \times d1 \times \dots\dots \times {d_n}^{w_n})^{\frac{1}{n}} \quad (15)$$

Where Hi, Li, w and n signify higher value, lower value, weight linked with a particular and number of performance measures respectively. The constraints for multi-objective optimization of Inconel 718 milling under MQL and NF-MQL lubrication environments have been given in Table 6. The achieved desirability with process parameters has been given in Table 7. It can be noticed when all performance measures have equal weights, desirability as high as 70.1% and 71.3% respectively can be attained for MQL and NF-MQL. The usefulness of NF-MQL over MQL has already been established in the preceding section and can be validated by comparison of performance measures values for maximum desirability of 71.3% and 70.1% from Table 7.

Table 6. Constraints for multi-objectiove optimization of performance measures

Name	Goal	Lower limit		Upper limit		Lower weight	Upper weight	Importance
		MQL	NF-MQL	MQL	NF- MQL			
Cutting speed	is in range	2000	2000	3000	3000	1	1	3
Feed rate	is in range	30	30	80	80	1	1	3
Depth of cut	is in range	0.3	0.3	0.8	0.8	1	1	3
Lubricant flow rate	is in range	400	400	800	800	1	1	3
Surface roughness	minimize	0.0625	0.049	0.296	0.24	1	1	3
Temperature	minimize	85	72	246	190	1	1	3
Material removal rate	maximize	39.6	39.6	1025.6	976.8	1	1	3
Power	minimize	295	380	1760	1660	1	1	3

Table 7. Achieved desirability for MQL and NF-MQL along with process parameters values

Sr. No.		S_P	F_R	D_{OC}	Fl_R	SR	T	MRR	P_C	Desirability	
MQL	1	2324	70	0.48	463	0.12	97.5	440	515.0	0.701	Selected
	2	2329	70	0.48	462	0.12	97.4	429	515.5	0.701	
NF-MQL	1	2364	71	0.44	427	0.10	85.7	432	504.3	0.713	Selected
	2	2365	72	0.43	424	0.11	85.6	431	504.8	0.710	

It can be observed that achievable ranges of performance measures for MQL lubrication environment are 0.06-0.30 μm for surface roughness, 85-246 °C for temperature, 40-1026 mm^3/min for material removal rate and 295-1760 watt for power (Table 6). However, with maximum desirability of 70.1%, 0.12 μm of surface roughness, 97.5 °C of temperature, 440 mm^3/min of material removal rate and 515 watts of power can only be achieved (Table 7). In the case of NF-MQL lubrication environment, achievable ranges of performance measures are 0.05-0.24 μm for surface roughness, 72-190 °C for temperature, 40-977 mm^3/min for material removal rate and 380-1660 watts for power (Table 6). However, with maximum desirability of 70%, 0.09 μm of surface roughness, 86 °C of temperature, 431 mm^3/min of material removal rate and 504 watts of power can only be attained (Table 7). Virtually on the shop floor, where machines reveal different ranges, floor shop planners have the constraints of a restricted variety of process parameters [41, 59]. For such circumstances, desirability plots (see Fig. 15(a, b)) can be used to select the available values of the machine with definite desirability function.

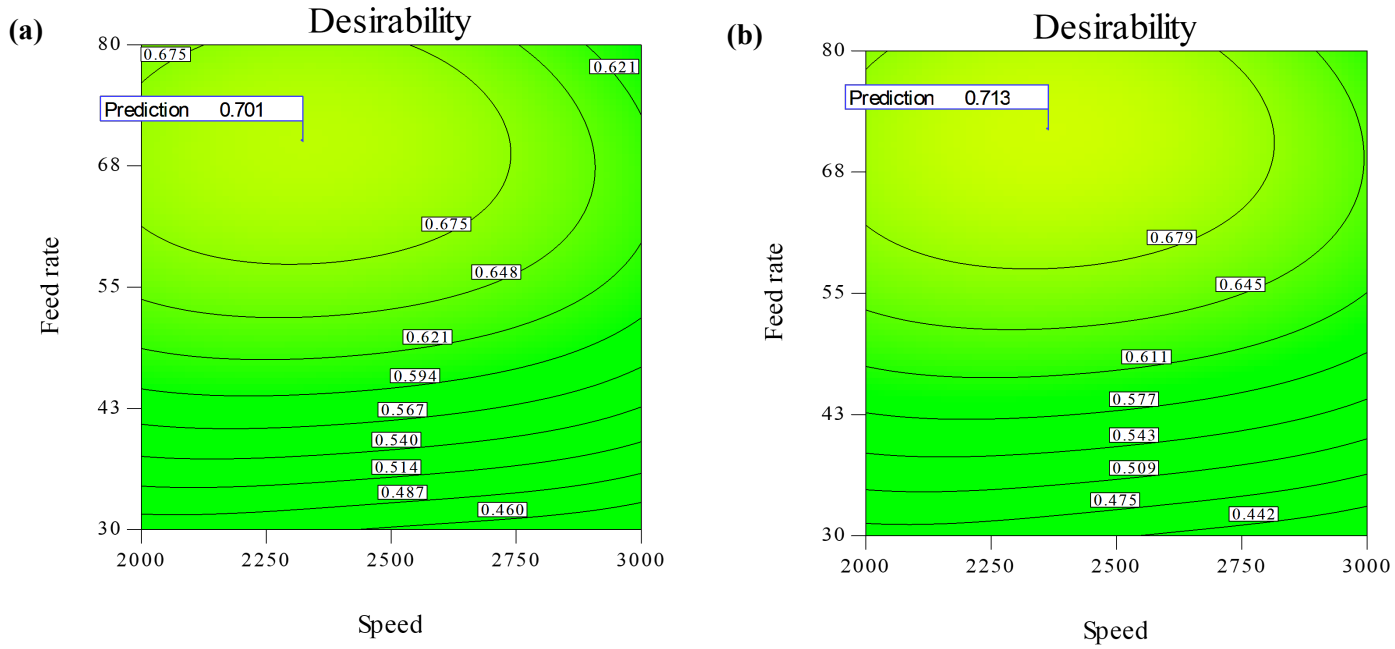

Figure 15. Desirability plots: (a) MQL milling, (b) NF-MQL milling

4. Conclusions

The aim of this research was to identify a sustainable production during face milling of Inconel 718 by using NF-MQL lubrication environment and MQL. The empirical models of SR, temperature, MRR and power were developed for both lubrication environments using RSM. Then, the comparison of both lubrication environments has been carried out. The sustainability was ensured through multi-objective optimization by enabling a compromise among; (i) productivity (MRR maximization), (ii) quality (SR and temperature minimization), and (iii) cost (power minimization). The conclusions of this research are as follows:

1. For both lubrication environments employed, depth of cut has been recognized as the most significant process parameter influencing SR, temperature, MRR and power.
2. Maximum MRR can be attained at high levels of depth of cut. Conversely, minimum SR, temperature and power can be accomplished at low levels of depth of cut.
3. By applying MQL lubrication environment and using the multi-objective optimization we have achieved desirability as high as 70.1% with a maximum material removal rate of 440 mm^3/min, minimum surface roughness 0.118 µm, temperature 97.5 °C and power 514.9 watts. In comparison, slightly higher desirability of 71.3% was achieved by applying NF-MQL lubrication environment with a maximum material removal rate of 432 mm^3/min, the minimum surface roughness of 0.092 µm, the temperature of 85.6 °C and power of 504.1 watts.

4. The comparison of the developed empirical models for both lubrication environments revealed that NF-MQL tends to decrease surface roughness, temperature and power by 20.1%, 14.7% and 13.3%, respectively with no comparable difference in material removal rate. Furthermore, by applying NF-MQL the surface roughness can be decreased to as low as 0.04 μm which is equivalent to manual polishing (a process very expensive for manufacturing industry).

The sustainability contour plots that have been developed can be utilized successfully within shop floor practitioners to attain higher degrees of desirability which suit their machines' limits.

Conflict of Interest

Authors declare no conflict of interest.

Author Contributions

Conceptualization, M.A.A. and M.U.F.; Data curation, M.A.H. and S.A.; Formal analysis, M.A.H., S.A. and A.W.; Funding acquisition, C.I.P.; Investigation, N.A.M., S.A. and A.W.; Methodology, M.A.A. and M.U.F.; Resources, A.W. and S.A.; Software, S.A. and M.A.H.; Writing—original draft, M.A.A., M.U.F. and M.A.H.; Writing—review & editing, M.A.A., M.U.F. and C.I.P. All authors have read and agreed to the published version of the manuscript.

Nomenclature

MQL	Minimum quantity lubrication
NF-MQL	Nanofluids based minimum quantity lubrication
SR	Surface roughness
P_C	Power consumption
ANOVA	Analysis of variance
CF	Cutting fluids
MRR	Material removal rate
T	Temperature
S_P	Speed
F_R	Feed rate
D_{OC}	Depth of cut
Fl_R	Flow rate
W_{bm}	Weight of the workpiece before machining
W_{am}	Weight of the workpiece after machining
CDGM	Combined desirability geometric mean
DOE	Design of experiment
CCD	Central composite design
RSM	Response surface methodology
k	Number of process variables
m	Center points
t_m	Machining time
ρ_w	Density of workpiece
SS	Sum of square
MS	Mean sum of square
df	Degree of freedom

di	Desirability identification
Yi	Performance measure
Hi	Higher value
Li	Lower value

References

1. Hegab H, Kishawy HA (2018) Towards sustainable machining of Inconel 718 using nano-fluid minimum quantity lubrication. Journal of Manufacturing and Materials Processing 2:50

2. Farooq MU, Hussain A, Masood T, Habib MS (2021) Supply Chain Operations Management in Pandemics: A State-of-the-Art Review Inspired by COVID-19. 13:2504

3. Darshan C, Jain S, Dogra M, et al (2019) Influence of dry and solid lubricant-assisted MQL cooling conditions on the machinability of Inconel 718 alloy with textured tool. The International Journal of Advanced Manufacturing Technology 105:1835–1849

4. Halim NHA, Haron CHC, Ghani JA, Azhar MF (2019) Tool wear and chip morphology in high-speed milling of hardened Inconel 718 under dry and cryogenic CO_2 conditions. Wear 426:1683–1690

5. Bai X, Zhou F, Li C, et al (2020) Physicochemical properties of degradable vegetable-based oils on minimum quantity lubrication milling. The International Journal of Advanced Manufacturing Technology 106:4143–4155

6. Khanna N, Agrawal C, Dogra M, Pruncu CI (2020) Evaluation of tool wear, energy consumption, and surface roughness during turning of inconel 718 using sustainable machining technique. Journal of Materials Research and Technology 9:5794-5804

7. Fontanive F, Zeilmann RP, Schenkel JD (2019) Surface quality evaluation after milling Inconel 718 with cutting edge preparation. The International Journal of Advanced Manufacturing Technology 104:1087–1098

8. Khanna N, Shah P (2020) Comparative analysis of dry, flood, MQL and cryogenic CO_2 techniques during the machining of 15-5-PH SS alloy. Tribology International 146:106196

9. Bennett EO (1983) Water based cutting fluids and human health. Tribology international 16:133–136

10. Said Z, Gupta M, Hegab H, et al (2019) A comprehensive review on minimum quantity lubrication (MQL) in machining processes using nano-cutting fluids. The International Journal of Advanced Manufacturing Technology 105:2057–2086

11. Bai X, Li C, Dong L, Yin Q (2019) Experimental evaluation of the lubrication performances of different nanofluids for minimum quantity lubrication (MQL) in milling Ti-6Al-4V. The International Journal of Advanced Manufacturing Technology 101:2621–2632

12. Ozcelik B, Kuram E, Cetin MH, Demirbas E (2011) Experimental investigations of vegetable based cutting fluids with extreme pressure during turning of AISI 304L. Tribology International 44:1864–1871

13. Wang X, Li C, Zhang Y, et al (2020) Vegetable oil-based nanofluid minimum quantity lubrication turning: Academic review and perspectives. Journal of Manufacturing Processes 59:76–97

14. Yin Q, Li C, Dong L, et al (2018) Effects of the physicochemical properties of different nanoparticles on lubrication performance and experimental evaluation in the NMQL milling of Ti–6Al–4V. The International Journal of Advanced Manufacturing Technology 99:3091–3109

15. Virdi RL, Chatha SS, Singh H (2020) Machining performance of Inconel-718 alloy under the influence of nanoparticles based minimum quantity lubrication grinding. Journal of Manufacturing Processes 59:355–365

16. Gupta MK, Song Q, Liu Z, et al (2020) Machining characteristics based life cycle assessment in eco-benign turning of pure titanium alloy. Journal of Cleaner Production 251:119598

17. Khan AM, Gupta MK, Hegab H, et al (2020) Energy-based cost integrated modelling and sustainability assessment of Al-GnP hybrid nanofluid assisted turning of AISI52100 steel. Journal of Cleaner Production 257:120502

18. Abellan-Nebot JV, Rogero MO (2019) Sustainable machining of molds for tile industry by minimum quantity lubrication. Journal of Cleaner Production 240:118082

19. Wang Y, Li C, Zhang Y, et al (2018) Processing characteristics of vegetable oil-based nanofluid MQL for grinding different workpiece materials. International Journal of Precision Engineering and Manufacturing-Green Technology 5:327–339

20. Rahmati B, Sarhan AA, Sayuti M (2014) Morphology of surface generated by end milling AL6061-T6 using molybdenum disulfide (MoS_2) nanolubrication in end milling machining. Journal of Cleaner Production 66:685–691

21. Jebaraj M, Pradeep Kumar M, Yuvaraj N, Mujibar Rahman G (2019) Experimental study of the influence of the process parameters in the milling of Al6082-T6 alloy. Materials and Manufacturing Processes 34:1411–1427

22. Do T-V, Le N-A-V (2019) Optimization of surface roughness and cutting force in MQL hard-milling of AISI H13 steel. In: Advances in Engineering Research and Application: Proceedings of the International Conference, ICERA 2018. Springer, pp 448–454

23. Singh G, Gupta MK, Mia M, Sharma VS (2018) Modeling and optimization of tool wear in MQL-assisted milling of Inconel 718 superalloy using evolutionary techniques. The International Journal of Advanced Manufacturing Technology 97:481–494

24. Varghese V, Ramesh MR, Chakradhar D (2018) Experimental investigation and optimization of machining parameters for sustainable machining. Materials and Manufacturing Processes 33:1782–1792

25. Cetin MH, Kilincarslan SK (2020) Effects of cutting fluids with nano-silver and borax additives on milling performance of aluminium alloys. Journal of Manufacturing Processes 50:170–182

26. Kitamura T, Tanaka R, Yamane Y, et al (2020) Performance evaluation method for cutting fluids using cutting force in micro-feed end milling. Precision Engineering 62:232–243

27. Yin Q, Li C, Zhang Y, et al (2018) Spectral analysis and power spectral density evaluation in Al_2O_3 nanofluid minimum quantity lubrication milling of 45 steel. The International Journal of Advanced Manufacturing Technology 97:129–145

28. Pham M-Q, Yoon H-S, Khare V, Ahn S-H (2014) Evaluation of ionic liquids as lubricants in micro milling–process capability and sustainability. Journal of cleaner production 76:167–173

29. Najiha MS, Rahman MM, Kadirgama K (2016) Performance of water-based TiO_2 nanofluid during the minimum quantity lubrication machining of aluminium alloy, AA6061-T6. Journal of cleaner production 135:1623–1636

30. Rao PN, Srikant RR (2015) Sustainable machining utilizing vegetable oil based nanofluids. In: 2015 International Conference on Smart Technologies and Management for Computing, Communication, Controls, Energy and Materials (ICSTM). IEEE, pp 664–672

31. Kole M, Dey TK (2013) Thermal performance of screen mesh wick heat pipes using water-based copper nanofluids. Applied Thermal Engineering 50:763–770

32. Ni C, Zhu L (2020) Investigation on machining characteristics of TC4 alloy by simultaneous application of ultrasonic vibration assisted milling (UVAM) and economical-environmental MQL technology. Journal of Materials Processing Technology 278:116518

33. AZOM Materials (2020) Material Directory | Materials Engineering. In: AZOM.com. https://www.azom.com/. Accessed 26 Jun 2020

34. Ross KNS, Manimaran G (2020) Machining Investigation of Nimonic-80A Superalloy Under Cryogenic CO_2 as Coolant Using PVD-TiAlN/TiN Coated Tool at 45° Nozzle Angle. Arab J Sci Eng 45:9267–9281. https://doi.org/10.1007/s13369-020-04728-8

35. Yıldırım ÇV, Kıvak T, Sarıkaya M, Erzincanlı F (2017) Determination of MQL Parameters Contributing to Sustainable Machining in the Milling of Nickel-Base Superalloy Waspaloy. Arab J Sci Eng 42:4667–4681. https://doi.org/10.1007/s13369-017-2594-z

36. Gao T, Li C, Zhang Y, et al (2019) Dispersing mechanism and tribological performance of vegetable oil-based CNT nanofluids with different surfactants. Tribology International 131:51–63

37. Nam JS, Kim DH, Chung H, Lee SW (2015) Optimization of environmentally benign micro-drilling process with nanofluid minimum quantity lubrication using response surface methodology and genetic algorithm. Journal of Cleaner Production 102:428–436

38. Hong SY, Markus I, Jeong W (2001) New cooling approach and tool life improvement in cryogenic machining of titanium alloy Ti-6Al-4V. International Journal of Machine Tools and Manufacture 41:2245–2260

39. Kim SW, Lee CM, Lee DW, et al (2001) Evaluation of the thermal characteristics in high-speed ball-end milling. Journal of Materials Processing Technology 113:406–409

40. Sealy MP, Liu ZY, Zhang D, et al (2016) Energy consumption and modeling in precision hard milling. Journal of Cleaner Production 135:1591–1601. https://doi.org/10.1016/j.jclepro.2015.10.094

41. Yan J, Li L (2013) Multi-objective optimization of milling parameters–the trade-offs between energy, production rate and cutting quality. Journal of Cleaner Production 52:462–471

42. Jamil M, Khan AM, Hegab H, et al (2020) Milling of Ti–6Al–4V under hybrid Al2O3-MWCNT nanofluids considering energy consumption, surface quality, and tool wear: a sustainable machining. The International Journal of Advanced Manufacturing Technology 107:4141–4157

43. Yıldırım ÇV, Kıvak T, Sarıkaya M, Şirin Ş (2020) Evaluation of tool wear, surface roughness/topography and chip morphology when machining of Ni-based alloy 625 under MQL, cryogenic cooling and CryoMQL. Journal of Materials Research and Technology 9:2079-2092

44. Hegab H, Umer U, Deiab I, Kishawy H (2018) Performance evaluation of Ti–6Al–4V machining using nano-cutting fluids under minimum quantity lubrication. The International Journal of Advanced Manufacturing Technology 95:4229–4241

45. An Q, Cai C, Zou F, et al (2020) Tool wear and machined surface characteristics in side milling Ti6Al4V under dry and supercritical CO_2 with MQL conditions. Tribology International 151:106511

46. An Q, Dang J (2020) Cooling effects of cold mist jet with transient heat transfer on high-speed cutting of titanium alloy. International Journal of Precision Engineering and Manufacturing-Green Technology 7:271–282

47. Nemetz AW, Daves W, Klünsner T, et al (2020) Experimentally validated calculation of the cutting edge temperature during dry milling of Ti6Al4V. Journal of Materials Processing Technology 278:116544

48. Gupta MK, Song Q, Liu Z, et al (2020) Experimental characterisation of the performance of hybrid cryo-lubrication assisted turning of Ti–6Al–4V alloy. Tribology International 153:106582

49. Shashidhara YM, Jayaram SR (2010) Vegetable oils as a potential cutting fluid—an evolution. Tribology international 43:1073–1081

50. Peña-Parás L, Maldonado-Cortés D, Rodríguez-Villalobos M, et al (2020) Enhancing tool life, and reducing power consumption and surface roughness in milling processes by nanolubricants and laser surface texturing. Journal of Cleaner Production 253:119836

51. Ibrahim AMM, Li W, Xiao H, et al (2020) Energy conservation and environmental sustainability during grinding operation of Ti–6Al–4V alloys via eco-friendly oil/graphene nano additive and MQL lubrication. Tribology International 106387

52. Chen Z, Zhou JM, Peng RL, et al (2018) Plastic Deformation and Residual Stress in High Speed Turning of AD730^{TM} Nickel-based Superalloy with PCBN and WC Tools. Procedia CIRP 71:440–445

53. Hegab H, Umer U, Soliman M, Kishawy HA (2018) Effects of nano-cutting fluids on tool performance and chip morphology during machining Inconel 718. The International Journal of Advanced Manufacturing Technology 96:3449–3458

54. Corrêa JG, Schroeter RB, Machado ÁR (2017) Tool life and wear mechanism analysis of carbide tools used in the machining of martensitic and supermartensitic stainless steels. Tribology International 105:102–117

55. Ali MA, Ishfaq K, Raza MH, et al (2020) Mechanical characterization of aged AA2026-AA2026 overcast joints fabricated by squeeze casting. The International Journal of Advanced Manufacturing Technology 107:3277-3297

56. Farooq MU, Ali MA, He Y, et al (2020) Curved profiles machining of Ti6Al4V alloy through WEDM: Investigations on geometrical errors. Journal of Materials Research and Technology 9:16186-16201

57. Hegab H, Kishawy HA, Gadallah MH, et al (2018) On machining of Ti-6Al-4V using multi-walled carbon nanotubes-based nano-fluid under minimum quantity lubrication. The International Journal of Advanced Manufacturing Technology 97:1593–1603

58. Niamat M, Sarfraz S, Ahmad W, et al (2020) Parametric modelling and multi-objective optimization of electro discharge machining process parameters for sustainable production. Energies, 13:38.

59. Cai C, Liang X, An Q, et al (2020) Cooling/Lubrication Performance of Dry and Supercritical CO 2-Based Minimum Quantity Lubrication in Peripheral Milling Ti-6Al-4V. International Journal of Precision Engineering and Manufacturing-Green Technology 1–17